

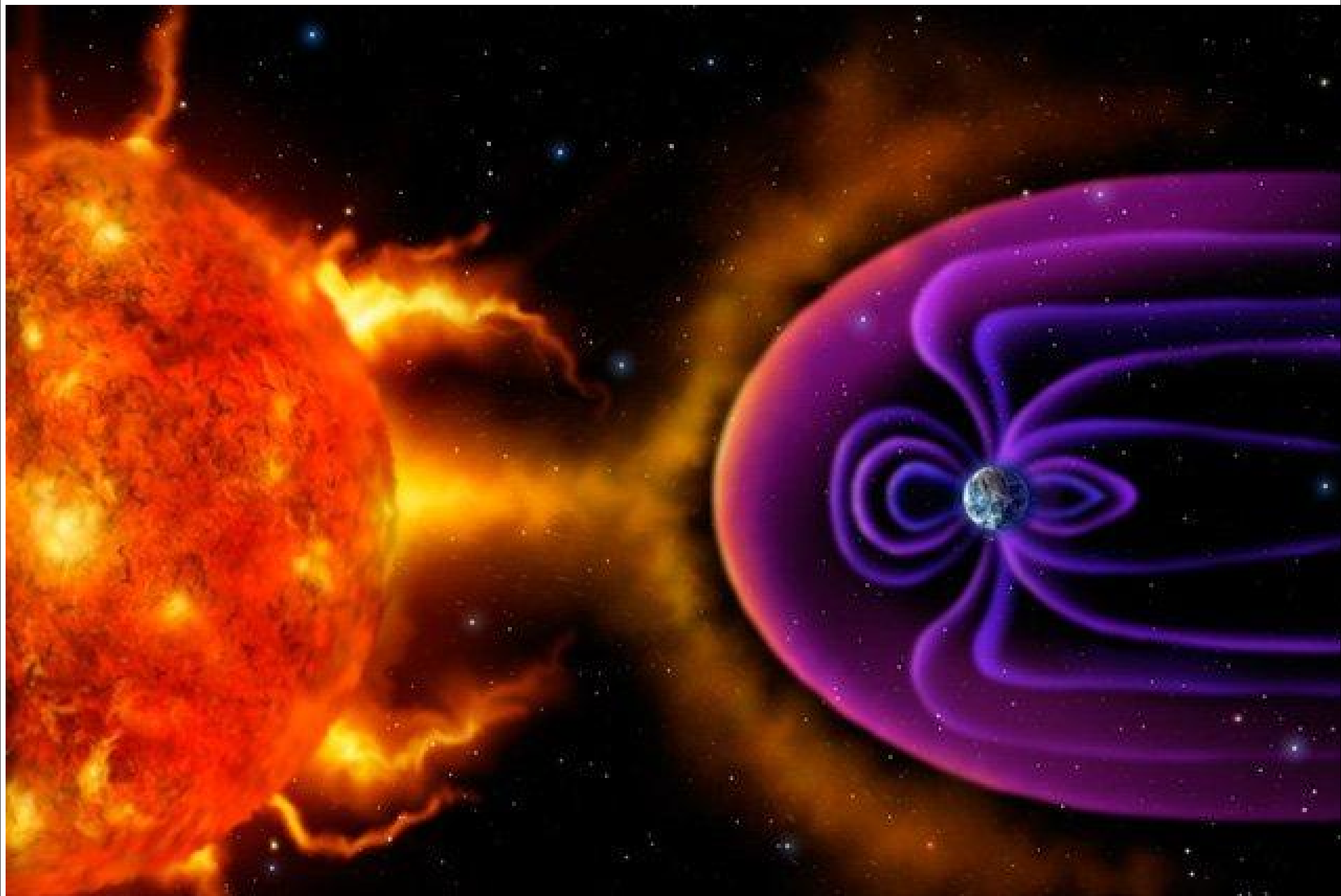
ON THE ORIGIN OF THE OPEN MAGNETIC FLUX PROBLEM IN HELIOSPHERE

M.L.Demidov
(ISTP SB RAS)

demid@iszf.irk.ru



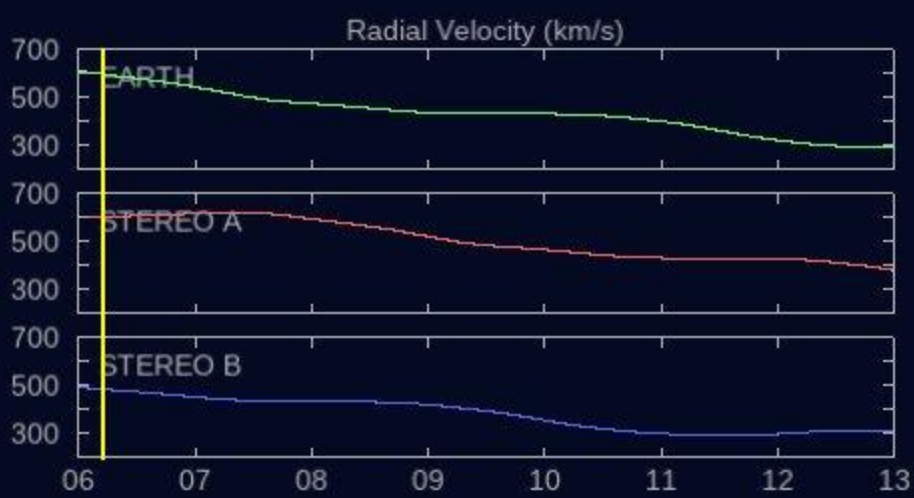
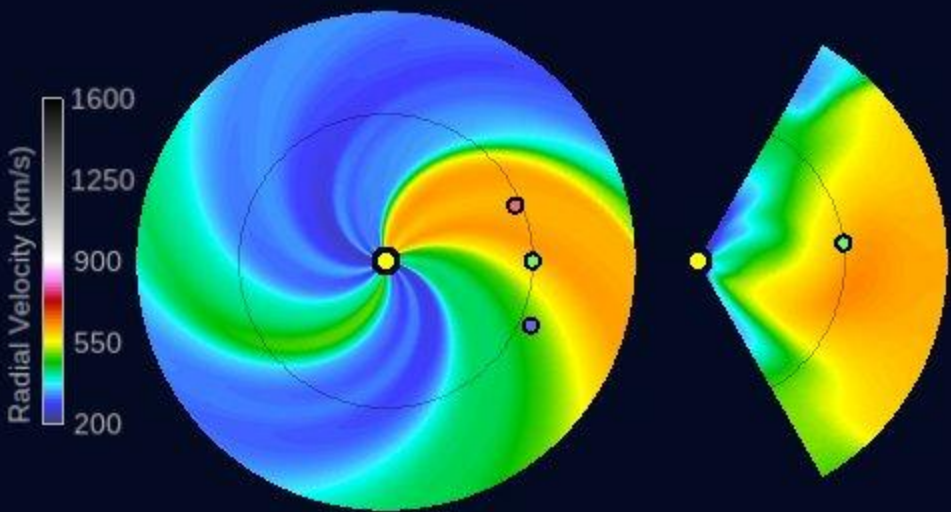
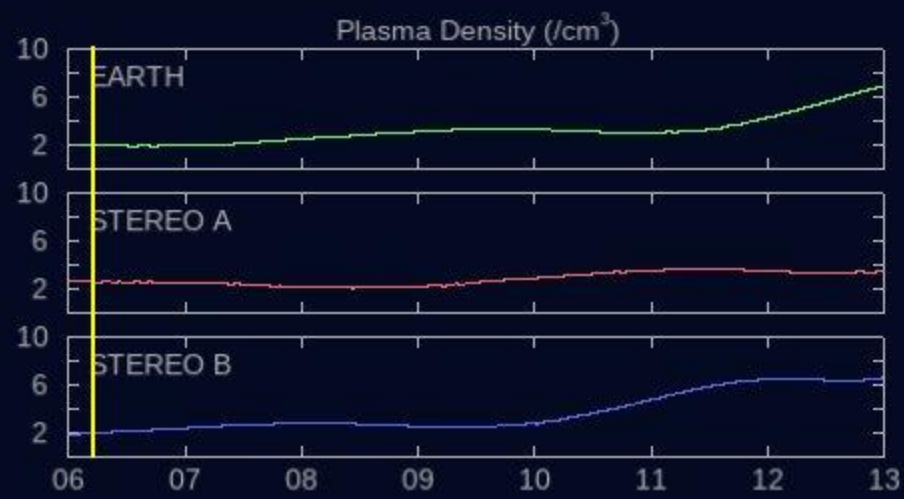
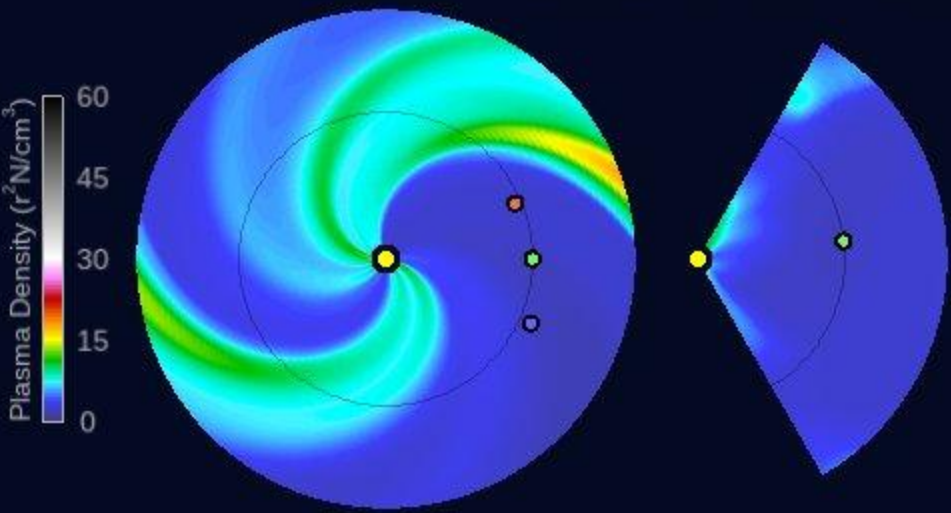
**The 15th Russian-Chinese Workshop on Space Weather
Irkutsk, 9 September 2024**



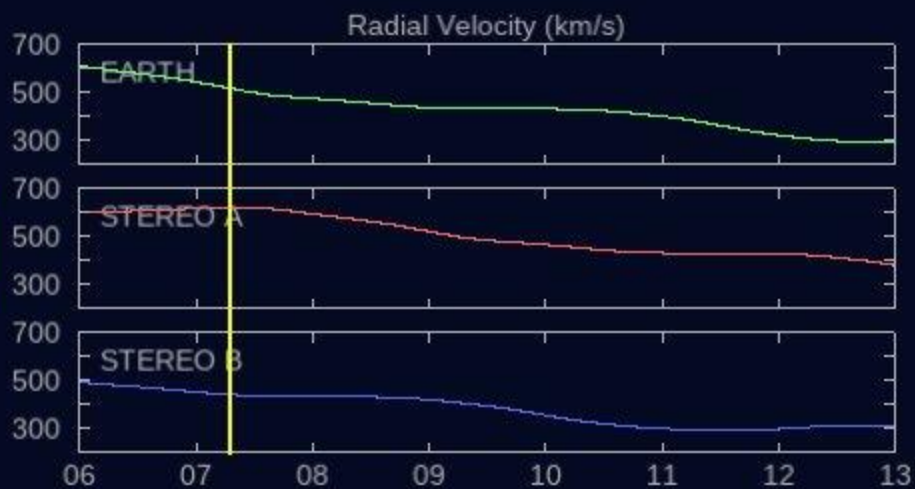
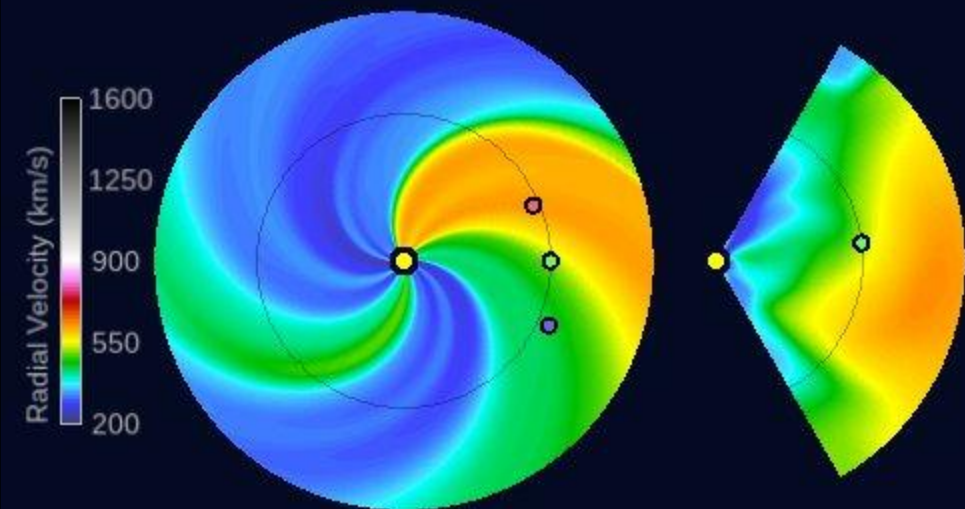
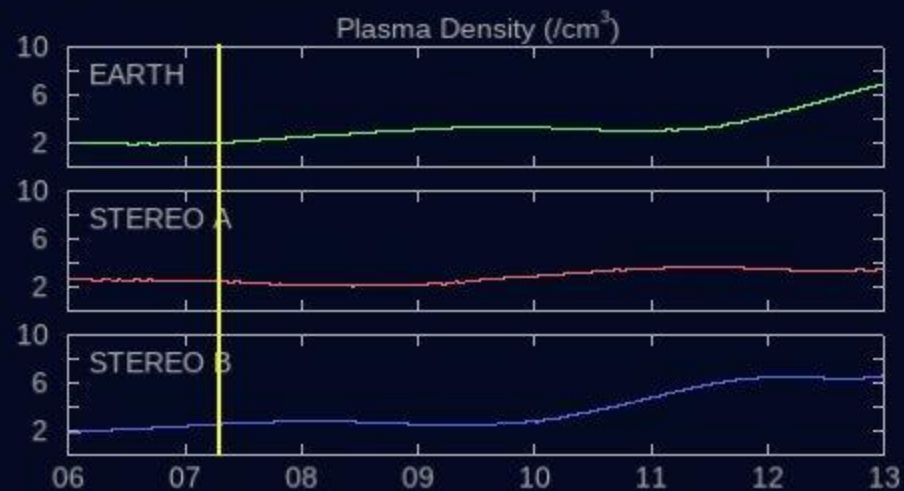
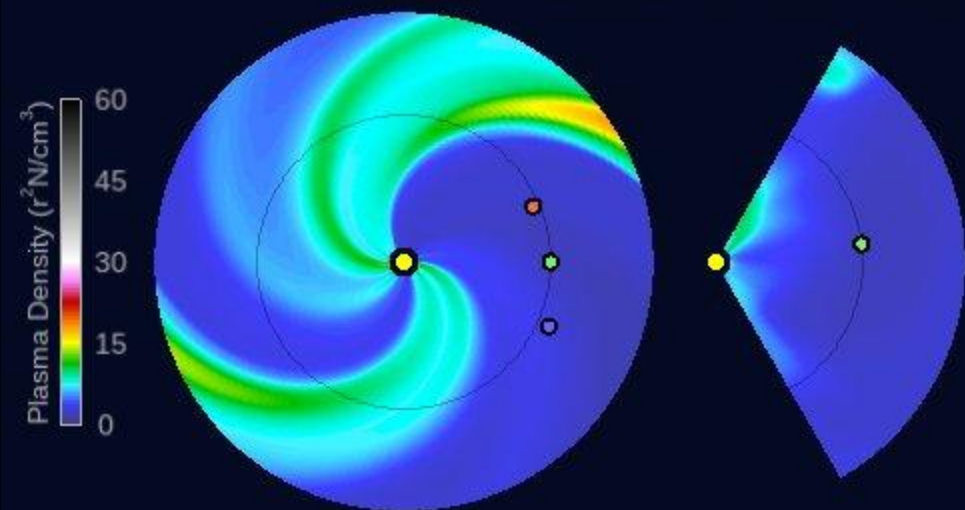
OUTLOOK

- **On the significance of space weather research for the modern science and technology**
- **Some of the main unsolved problems of the space weather predictions based on measurements of solar magnetic fields**
- **The open magnetic flux problem in historical aspect**
- **Ulrich's and Ulrich's et al papers concerning recalibration of observations in the FeI 525.0 nm spectral line**
- **Results based on spectropolarimetric observations with STOP telescope**
- **Conclusions**
-

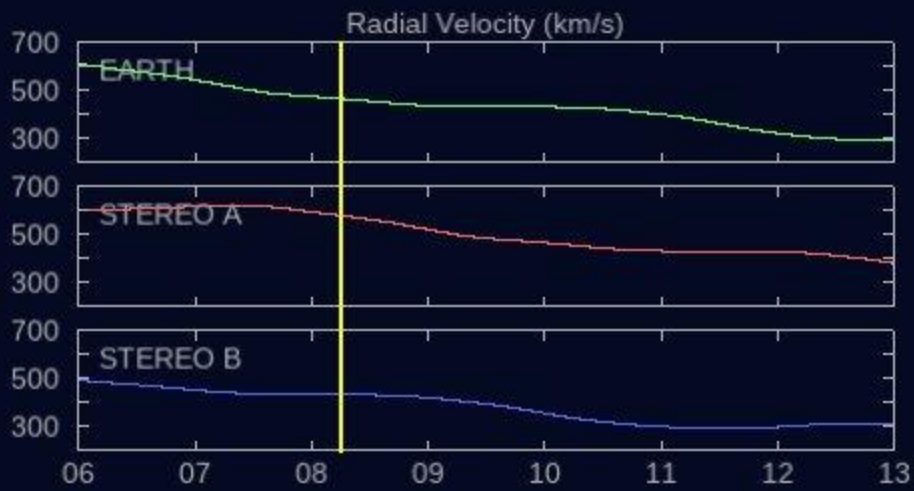
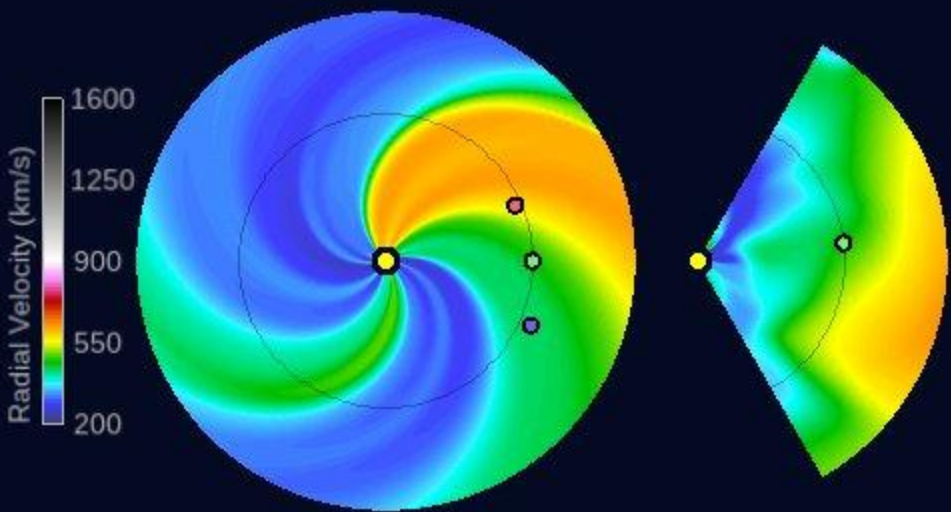
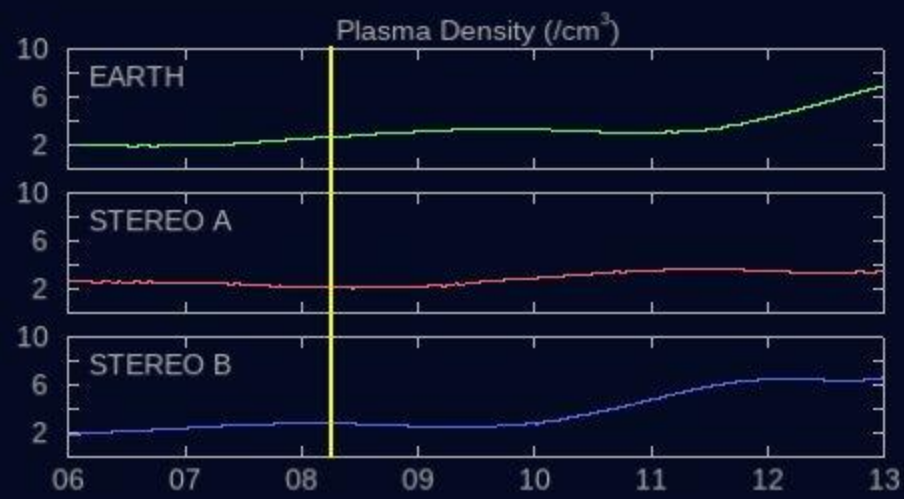
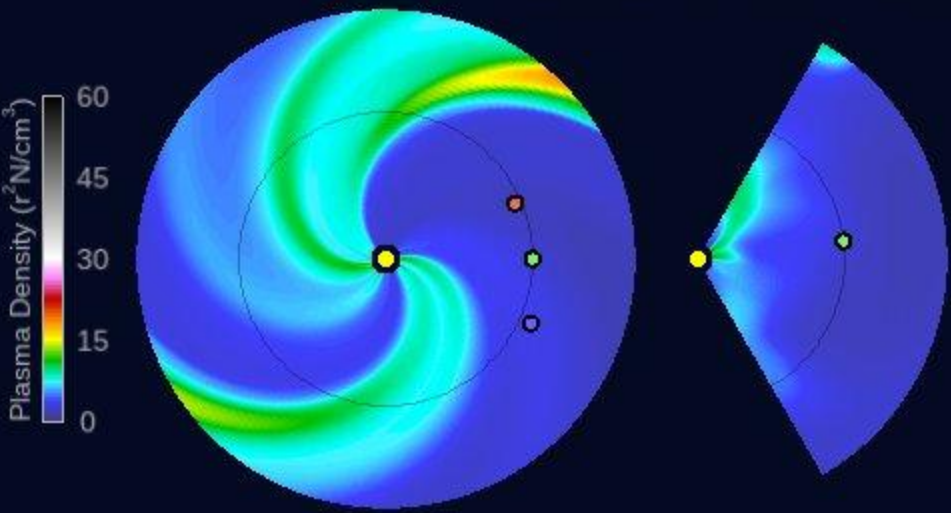
2024-09-06 05:00:00



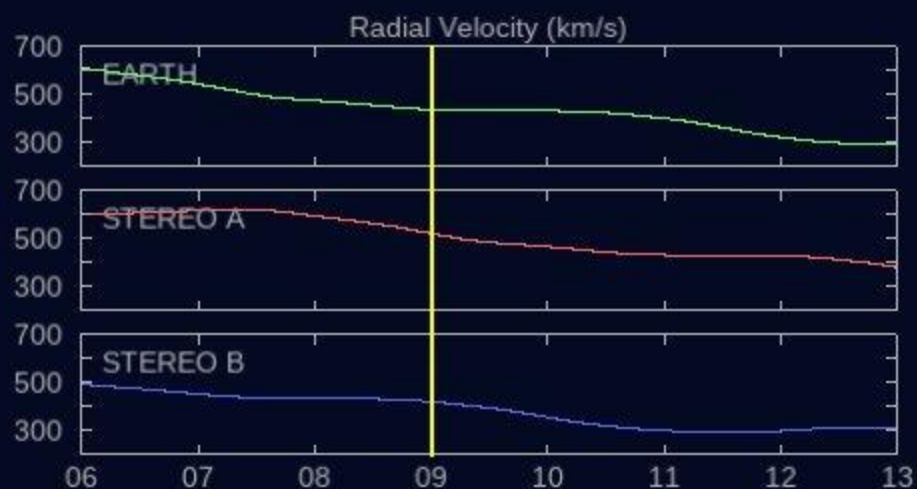
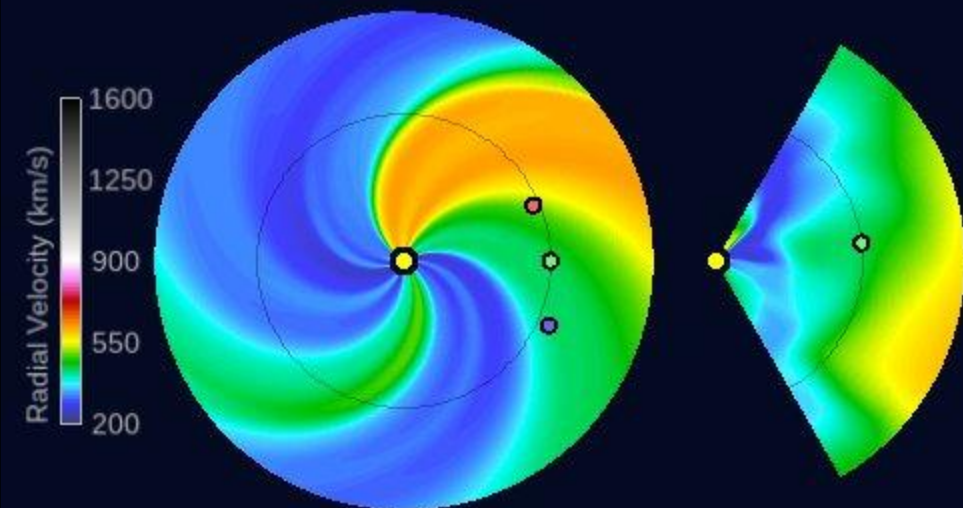
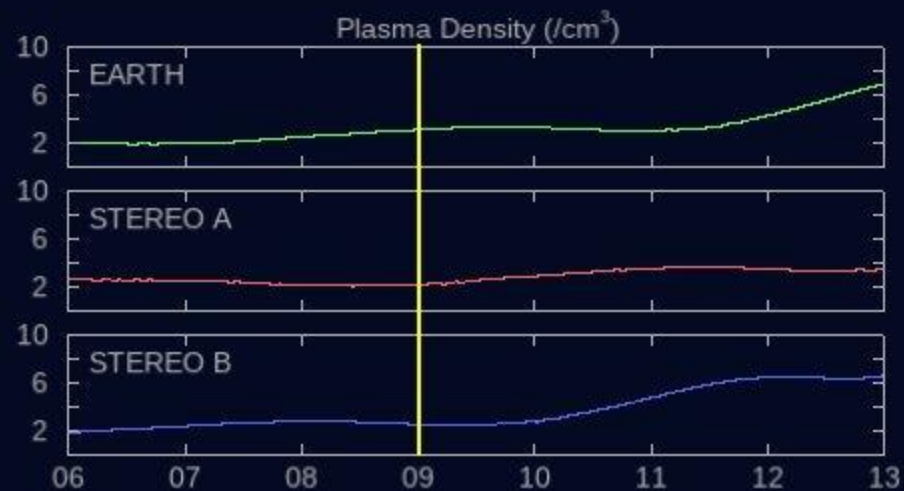
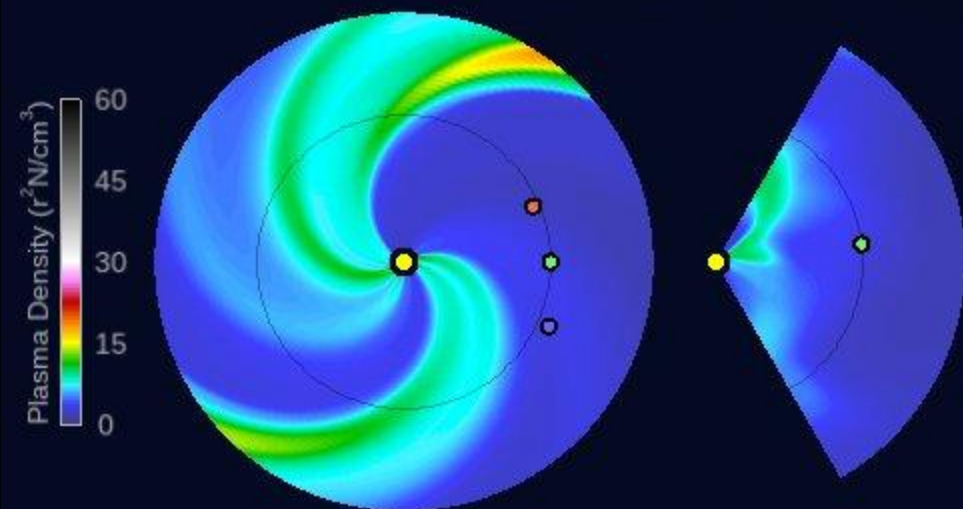
2024-09-07 07:00:00



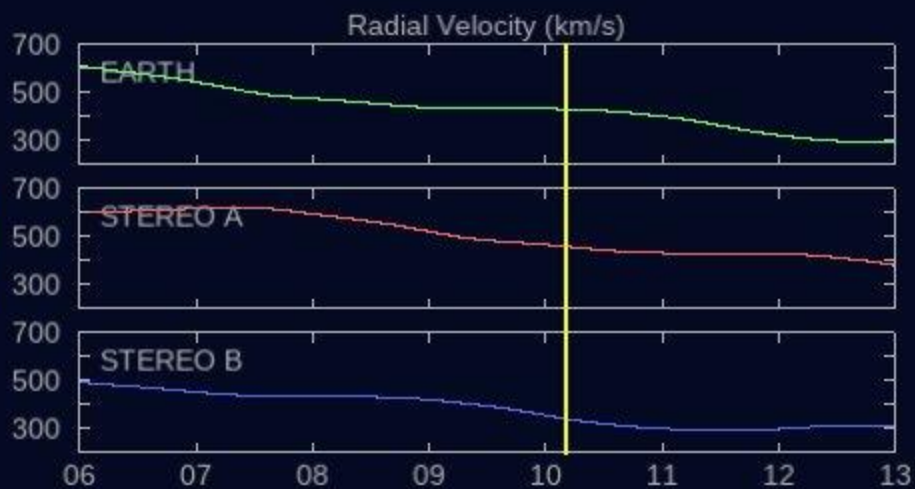
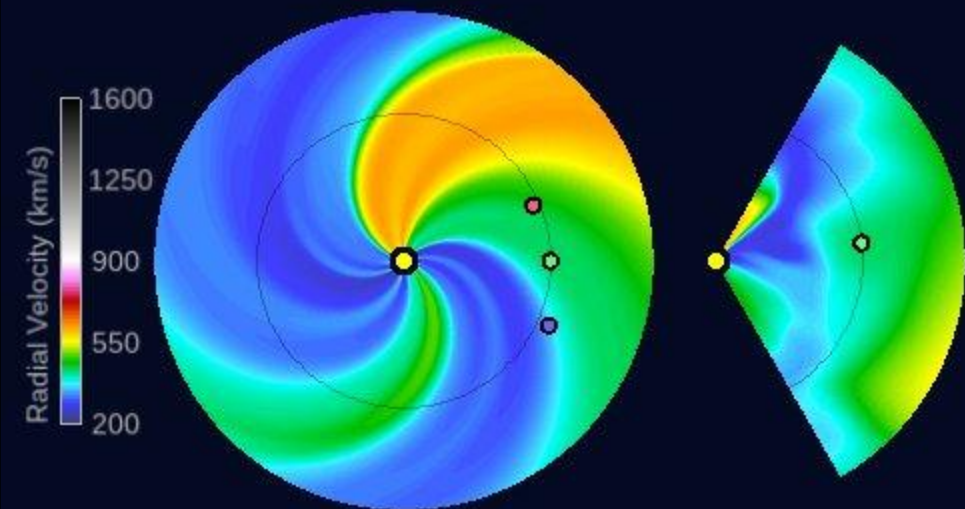
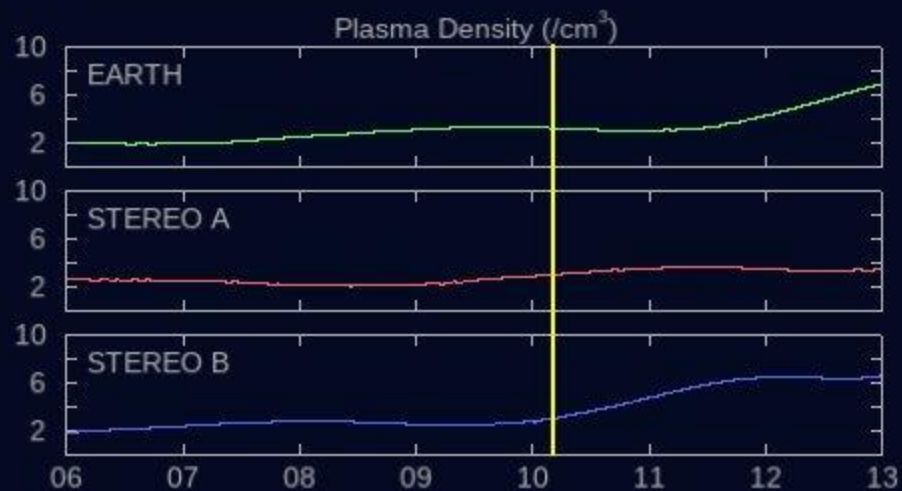
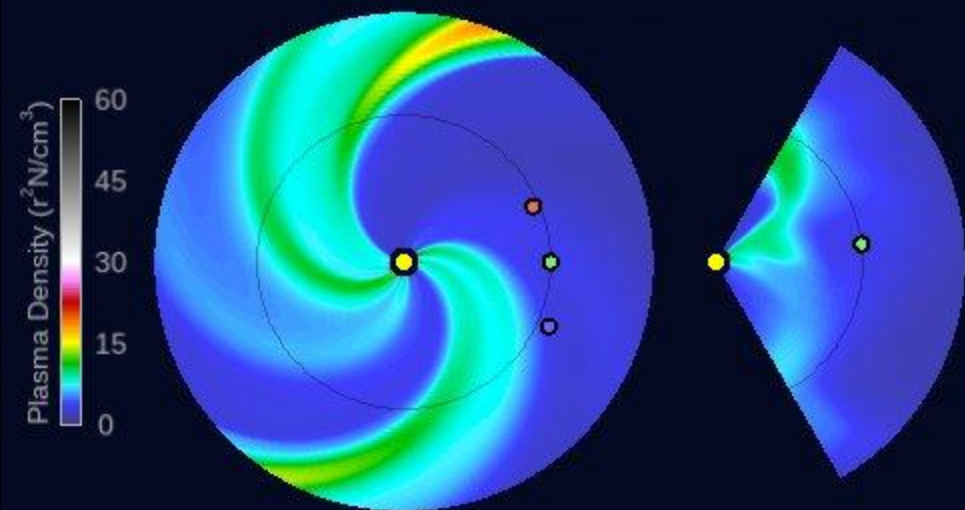
2024-09-08 06:00:00



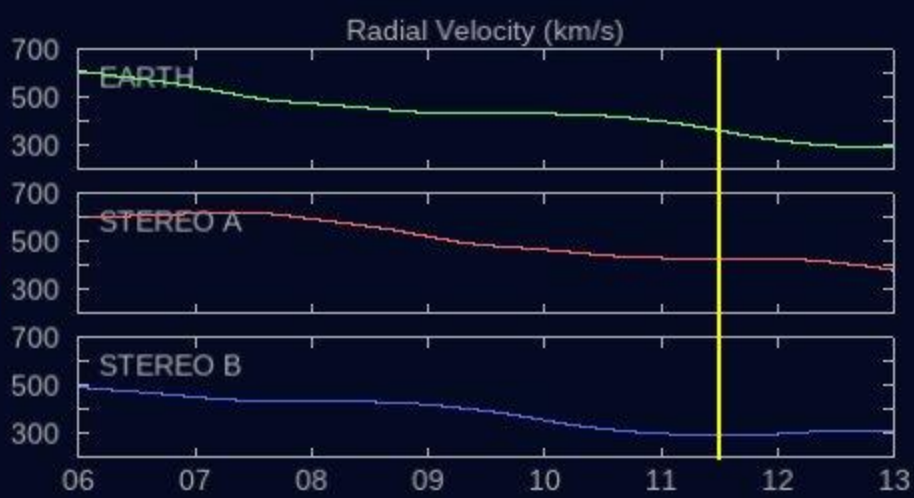
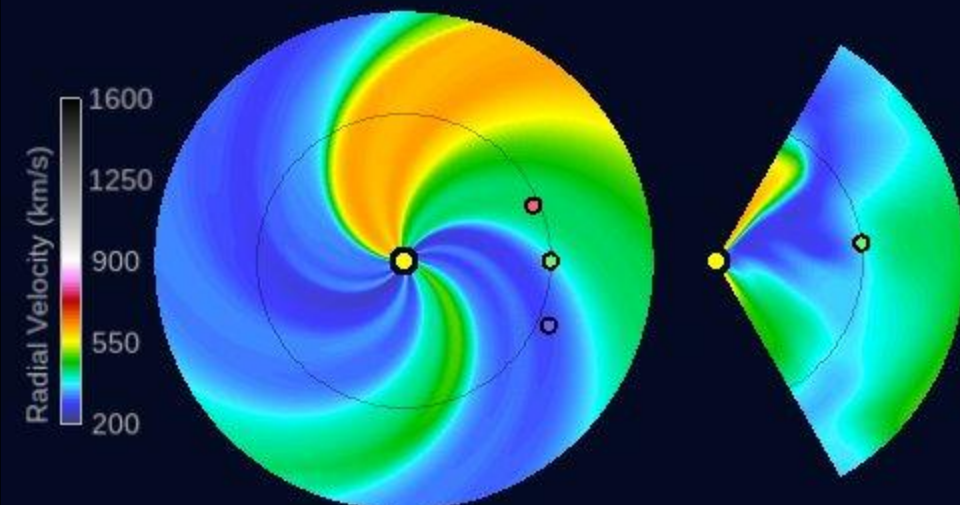
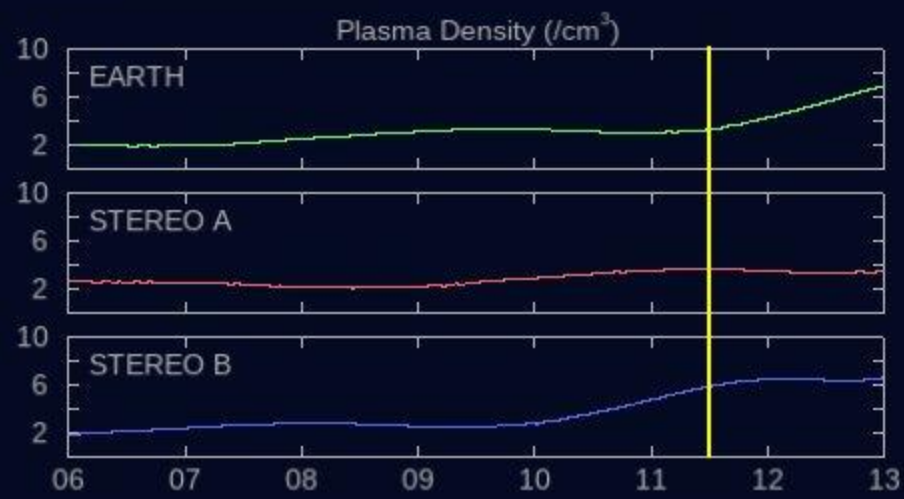
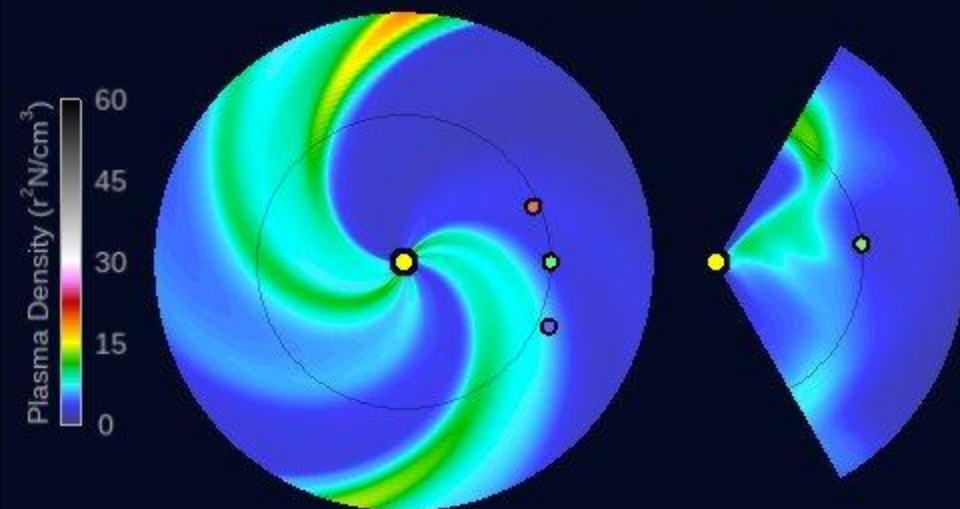
2024-09-09 00:00:00



2024-09-10 04:00:00



2024-09-11 12:00:00



Space Weather



RESEARCH ARTICLE

10.1029/2020SW002499

Key Points:

- Alternative methods to the Wang-Sheeley-Argé model were tested to predict solar wind speed, density, and magnetic field magnitude at Earth
- Predictions at Earth are to a large part controlled by the coronal model and ENLIL inner boundary conditions
- IPS tomographic analysis of the heliosphere can be used to adequately simulate the solar wind speed and density at Earth

Correspondence to:

S. Gonzi,
siegfried.gonzi@metoffice.gov.uk

Citation:

Gonzi, S., Weinzierl, M., Bocquet, F.-X., Bisi, M. M., Odstrcil, D., Jackson, B. V., et al. (2021). Impact of inner heliospheric boundary conditions on solar wind predictions at Earth. *Space Weather*, 19, e2020SW002499. <https://doi.org/10.1029/2020SW002499>

Received 12 MAR 2020

Accepted 19 AUG 2020

Accepted article online 21 AUG 2020

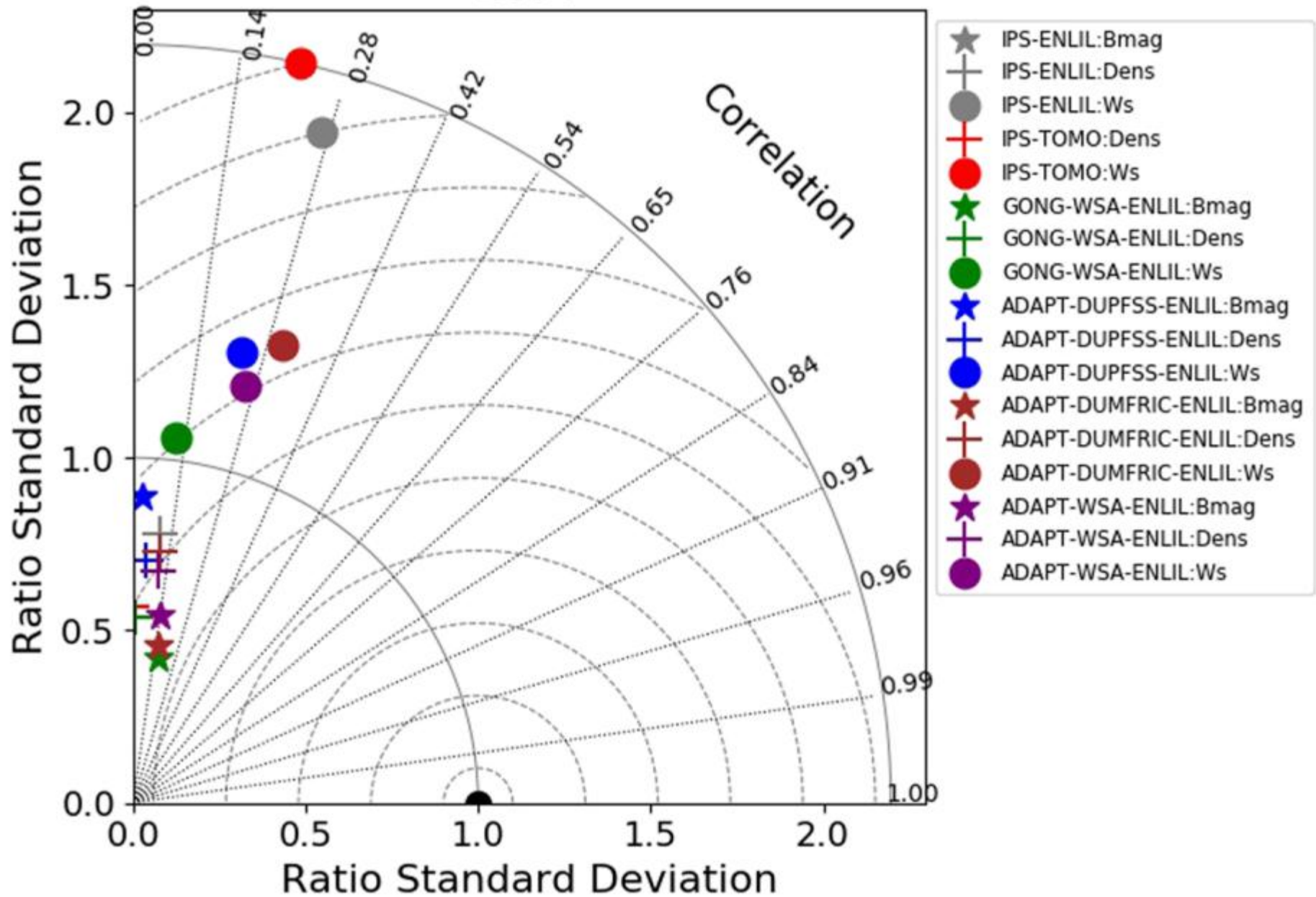
Impact of Inner Heliospheric Boundary Conditions on Solar Wind Predictions at Earth

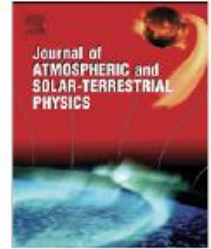
Siegfried Gonzi¹ , M. Weinzierl², F.-X. Bocquet³, M. M. Bisi⁴ , D. Odstrcil⁵, B. V. Jackson⁶ , A. R. Yeates⁷ , D. R. Jackson¹ , C. J. Henney⁸ , and C. Nick Arge⁹

¹Met Office, Exeter, UK, ²Advanced Research Computing, University of Durham, Durham, UK, ³Spire Global UK Limited, Glasgow, UK, ⁴Science and Technology Facilities Council, RAL Space, Didcot, UK, ⁵Space Weather Lab, George Mason University, Fairfax, VA, USA, ⁶Center for Astrophysics and Space Sciences, University of California, San Diego, La Jolla, CA, USA, ⁷Department of Mathematical Sciences, University of Durham, Durham, UK, ⁸Space Vehicles Directorate, Air Force Research Laboratory, Kirtland AFB, NM, USA, ⁹NASA Goddard Space Flight Center, Greenbelt, MD, USA

Abstract Predictions of the physical parameters of the solar wind at Earth are at the core of operational space weather forecasts. Such predictions typically use line-of-sight observations of the photospheric magnetic field to drive a heliospheric model. The models Wang-Sheeley-Argé (WSA) and ENLIL for the transport in the heliosphere are commonly used for these respective tasks. Here we analyze the impact of replacing the potential field coronal boundary conditions from WSA with two alternative approaches. The first approach uses a more realistic nonpotential rather than potential approach, based on the Durham Magneto Frictional Code (DUMFRIC) model. In the second approach the ENLIL inner boundary conditions are based on Inter Planetary Scintillation observations (IPS). We compare predicted solar wind speed, plasma density, and magnetic field magnitude with observations from the WIND spacecraft for two 6-month intervals in 2014 and 2016. Results show that all models tested produce fairly similar output when compared to the observed time series. This is not only reflected in fairly low correlation coefficients (<0.3) but also large biases. For example, for solar wind speed some models have average biases of more than 150 km/s. On a positive note, the choice of coronal magnetic field model has a clear influence on the model results when compared to the other models in this study. Simulations driven by IPS data have a high success rate with regard to detection of the high speed solar wind. Our results also indicate that model forecasts do not degrade for longer forecast times.

2014





Underestimates of magnetic flux in coupled MHD model solar wind solutions

Michael L. Stevens^{a,*}, Jon A. Linker^b, Pete Riley^b, W. Jeffrey Hughes^c

^a *Harvard Smithsonian Center for Astrophysics, 60 Garden Street, Cambridge, MA, United States*

^b *Predictive Science, Inc, 9990 Mesa Rim Road, San Diego, CA, United States*

^c *Boston University, 1 University Road, Boston, MA, United States*

ARTICLE INFO

Article history:

Received 10 September 2011

Received in revised form

31 January 2012

Accepted 6 February 2012

Available online 14 February 2012

Keywords:

Corona

Solar wind

Corotating interaction regions

Magnetohydrodynamics






Space weather

ABSTRACT

When validated with spacecraft observations, one enduring characteristic of global MHD solar wind models is the tendency to underestimate the interplanetary magnetic flux. This study quantifies the “missing flux” problem for models used in the coordinated Center for Integrated Space Weather Modeling study of corotating interaction regions, and identifies the model parameters most strongly related to the effect. We show that two important contributions are (1) insufficient thermal pressure in the coronal model to extract the required magnetic flux and (2) numerical diffusion in the model current sheets. Using Ulysses observations, we derive a calibration for the effective temperature in the polytropic coronal Magnetohydrodynamics Around a Sphere model that produces the expected interplanetary field at high latitudes. After recalibrating, we find that a 40% discrepancy still remains in the ecliptic plane. Moreover, the problem is 5% more severe for models of the solar cycle 23 minimum than it is for models of the cycle 22 minimum. We argue that the resolution of the heliospheric current sheet strongly affects both the general underestimate and the discrepancy between the two cycles. We also argue that improved resolution of current sheets in the low corona will further reduce the effect.



The Open Flux Problem

J. A. Linker¹, R. M. Caplan¹ , C. Downs¹, P. Riley¹, Z. Mikic¹, R. Lionello¹ ,
C. J. Henney², C. N. Arge³, Y. Liu⁴, M. L. Derosa⁵ , A. Yeates⁶ , and M. J. Owens⁷ 

¹Predictive Science Inc., 9990 Mesa Rim Road, Suite 170, San Diego, CA 92121, USA; linkerj@predsci.com

²Air Force Research Lab/Space Vehicles Directorate, 3550 Aberdeen Avenue SE, Kirtland AFB, NM, USA

³Science & Exploration Directorate, NASA/GSFC, Greenbelt, MD 20771, USA

⁴W. W. Hansen Experimental Physics Laboratory, Stanford University, Stanford, CA 94305, USA

⁵Lockheed Martin Solar and Astrophysics Laboratory, 3251 Hanover Street B/252, Palo Alto, CA 94304, USA

⁶Department of Mathematical Sciences, Durham University, Durham, DH1 3LE, UK

⁷Space and Atmospheric Electricity Group, Department of Meteorology, University of Reading, Earley Gate, P.O. Box 243, Reading RG6 6BB, UK

Received 2017 August 7; revised 2017 September 1; accepted 2017 September 2; published 2017 October 12

Abstract

The heliospheric magnetic field is of pivotal importance in solar and space physics. The field is rooted in the Sun's photosphere, where it has been observed for many years. Global maps of the solar magnetic field based on full-disk magnetograms are commonly used as boundary conditions for coronal and solar wind models. Two primary observational constraints on the models are (1) the open field regions in the model should approximately correspond to coronal holes (CHs) observed in emission and (2) the magnitude of the open magnetic flux in the model should match that inferred from in situ spacecraft measurements. In this study, we calculate both magnetohydrodynamic and potential field source surface solutions using 14 different magnetic maps produced from five different types of observatory magnetograms, for the time period surrounding 2010 July. We have found that for all of the model/map combinations, models that have CH areas close to observations underestimate the interplanetary magnetic flux, or, conversely, for models to match the interplanetary flux, the modeled open field regions are larger than CHs observed in EUV emission. In an alternative approach, we estimate the open magnetic flux entirely from solar observations by combining automatically detected CHs for Carrington rotation 2098 with observatory synoptic magnetic maps. This approach also underestimates the interplanetary magnetic flux. Our results imply that either typical observatory maps underestimate the Sun's magnetic flux, or a significant portion of the open magnetic flux is not rooted in regions that are obviously dark in EUV and X-ray emission.



Estimating Total Open Heliospheric Magnetic Flux

S. Wallace^{1,2} · C.N. Arge² · M. Pattichis³ ·
R.A. Hock-Mysliwiec⁴ · C.J. Henney⁴

Received: 19 October 2018 / Accepted: 11 January 2019 / Published online: 8 February 2019
© Springer Nature B.V. 2019

Abstract Over the solar-activity cycle, there are extended periods where significant discrepancies occur between the spacecraft-observed total (unsigned) open magnetic flux and that determined from coronal models. In this article, the total open heliospheric magnetic flux is computed using two different methods and then compared with results obtained from *in-situ* interplanetary magnetic-field observations. The first method uses two different types of photospheric magnetic-field maps as input to the Wang–Sheeley–Arge (WSA) model: i) traditional Carrington or diachronic maps, and ii) Air Force Data Assimilative Photospheric Flux Transport model synchronic maps. The second method uses observationally derived helium and extreme-ultraviolet coronal-hole maps overlaid on the same magnetic-field maps in order to compute total open magnetic flux. The diachronic and synchronic maps are both constructed using magnetograms from the same source, namely the National Solar Observatory *Kitt Peak Vacuum Telescope* and *Vector Spectromagnetograph*. The results of this work show that the total open flux obtained from observationally derived coronal holes agrees remarkably well with that derived from WSA, especially near solar minimum. This suggests that, on average, coronal models capture well the observed large-scale coronal-hole structure over most of the solar cycle. Both methods show considerable deviations from total open flux deduced from spacecraft data, especially near solar maximum, pointing to something other than poorly determined coronal-hole area specification as the source of these discrepancies.

Keywords Magnetic fields, interplanetary · Coronal holes · Corona, models



Improving Coronal Hole Detections and Open Flux Estimates

Ronald M. Caplan , Emily I. Mason , Cooper Downs , and Jon A. Linker 

Predictive Science Inc., 9990 Mesa Rim Road, Suite 170, San Diego, CA 92121, USA; caplanr@predsci.com

Received 2023 May 22; revised 2023 September 29; accepted 2023 October 7; published 2023 November 10

Abstract

One systematic limitation of solar coronal hole (CH) detection at extreme ultraviolet (EUV) wavelengths is the obscuration of dark regions of the corona by brighter structures along the line of sight. Another problem arises when using CHs to compute the Sun's open magnetic flux, where surface measurements of the radial magnetic field, B_r^\odot , are situated slightly below the effective height of coronal EUV emission. In this paper, we explore these two limitations utilizing a thermodynamic magnetohydrodynamic (MHD) model of the corona for Carrington rotation (CR) 2101, where we generate CH detections from EUV 193 Å images of the corona forward-modeled from the MHD solution, and where the modeled open field is known. We demonstrate a method to combine EUV images into a full Sun map that helps alleviate CH obscuration called the *minimum intensity disk merge* (MIDM). We also show the variation in measured open flux and CH area that is due to the effective height differences between EUV and B_r^\odot measurements. We then apply the MIDM method to SDO/AIA 193 Å observations from CR 2101, and conduct an analogous analysis. In this case, the MIDM method uses time-varying images, the effects of which are discussed. We show that overall, the MIDM method and an appreciation of the effective height mismatch provide a useful new way to extract a broader view of CHs, especially near the poles. In turn, they enable improved estimates of the open magnetic flux, and help facilitate comparisons between models and observations.

Unified Astronomy Thesaurus concepts: [Solar corona \(1483\)](#); [Solar coronal holes \(1484\)](#); [Solar surface \(1527\)](#); [Astronomy software \(1855\)](#); [Astronomy data analysis \(1858\)](#)

The Open Flux Problem: The Need for High Latitude Observations

First Author: Jon A. Linker

Predictive Science Inc., San Diego, CA

Co-Authors: Pete Riley¹, Cooper Downs¹, Ronald M. Caplan¹, Craig Deforest², Sarah E Gibson³, Donald M Hassler², J Todd Hoeksema⁴, W. Dean Pesnell⁵, Xudong Sun⁶, Nicholeen M. Viall⁵

¹Predictive Science Inc., San Diego, CA

²Southwest Research Institute, Boulder, CO

³National Center for Atmospheric Research, High Altitude Observatory, Boulder, CO

⁴Stanford University, HEPL, Stanford, CA

⁵NASA Goddard Space Flight Center, Greenbelt, MD

⁶University of Hawaii at Manoa, Institute for Astronomy, Honolulu, HI

Synopsis

The Sun's open magnetic field is a fundamental aspect of coronal and heliospheric physics. The primary source location of the open magnetic field is believed to be coronal holes, usually detected by the absence of EUV and/or X-ray emission. We have observed photospheric magnetic fields remotely and measured interplanetary magnetic fields in situ for over five decades. A long-standing issue is that models based on photospheric magnetic field observations significantly underestimate the open magnetic field inferred from interplanetary measurements, if their open field regions are compatible with coronal hole observations. This is not a model problem, but rather an observed open flux problem: When the open flux is estimated from coronal hole detections superimposed on observatory-based solar magnetic flux maps (entirely eliminating models), the deficit persists or is even larger. A major uncertainty is the strength of the polar magnetic fields, which are poorly observed from the ecliptic plane. Resolving the contribution of polar fields requires line-of-sight measurements of the photospheric field at high heliographic latitude (greater than 65°) with corresponding detection of coronal hole boundaries in a coronal emission line, at a time not too far from solar minimum (when polar fields are strongest), for at least a solar rotation. Regardless of the result (strong or weak polar fields), such measurements will have profound implications for our understanding of the structure of the solar corona and inner heliosphere, including CME and SEP propagation, and the formation and sources of the solar wind.



On the Origin of the Sudden Heliospheric Open Magnetic Flux Enhancement During the 2014 Pole Reversal

Stephan G. Heinemann¹ , Mathew J. Owens² , Manuela Temmer³ , James A. Turtle⁴, Charles N. Arge⁵ , Carl J. Henney⁶ , Jens Pomoell¹ , Eleanna Asvestari¹ , Jon A. Linker⁴ , Cooper Downs⁴ , Ronald M. Caplan⁴ , Stefan J. Hofmeister⁷ , Camilla Scolini^{8,9} , Rui F. Pinto¹⁰ , and Maria S. Madjarska^{11,12}

¹ Department of Physics, University of Helsinki, P.O. Box 64, 00014, Helsinki, Finland; stephan.heinemann@hmail.at

² Space and Atmospheric Electricity Group, Department of Meteorology, University of Reading, Earley Gate, P.O. Box 243, Reading, RG6 6BB, UK

³ Institute of Physics, University of Graz, Universitätsplatz 5, 8010 Graz, Austria

⁴ Predictive Science Inc., 9990 Mesa Rim Road, Suite 170, San Diego, CA 92121, USA

⁵ Heliophysics Science Division, NASA Goddard Space Flight Center, Code 671, Greenbelt, MD 20771, USA

⁶ Air Force Research Laboratory, Space Vehicles Directorate, KAFB, NM 87117, USA

⁷ Leibniz-Institute for Astrophysics Potsdam, An der Sternwarte 16, 14482 Potsdam, Germany

⁸ Institute for the Study of Earth, Oceans, and Space, University of New Hampshire, Durham, NH 03824, USA

⁹ Solar–Terrestrial Centre of Excellence–SIDC, Royal Observatory of Belgium, 1180 Uccle, Belgium

¹⁰ IRAP, Université de Toulouse; UPS-OMP; CNRS, 9 Av. colonel Roche, BP 44346, F-31028 Toulouse cedex 4, France

¹¹ Max-Planck-Institut für Sonnensystemforschung, Justus-von-Liebig-Weg 3, 37077 Göttingen, Germany

¹² Space Research and Technology Institute, Bulgarian Academy of Sciences, Acad. Georgy Bonchev Str., Bl. 1, 1113, Sofia, Bulgaria

Received 2023 November 10; revised 2024 February 16; accepted 2024 February 19; published 2024 April 16

Abstract

Coronal holes are recognized as the primary sources of heliospheric open magnetic flux (OMF). However, a noticeable gap exists between in situ measured OMF and that derived from remote-sensing observations of the Sun. In this study, we investigate the OMF evolution and its connection to solar structures throughout 2014, with special emphasis on the period from September to October, where a sudden and significant OMF increase was reported. By deriving the OMF evolution at 1 au, modeling it at the source surface, and analyzing solar photospheric data, we provide a comprehensive analysis of the observed phenomenon. First, we establish a strong correlation between the OMF increase and the solar magnetic field derived from a potential-field source-surface model ($cc_{\text{Pearson}} = 0.94$). Moreover, we find a good correlation between the OMF and the open flux derived from solar coronal holes ($cc_{\text{Pearson}} = 0.88$), although the coronal holes only contain 14%–32% of the Sun's total open flux. However, we note that while the OMF evolution correlates with coronal hole open flux, there is no correlation with the coronal hole area evolution ($cc_{\text{Pearson}} = 0.0$). The temporal increase in OMF correlates with the vanishing remnant magnetic field at the southern pole, caused by poleward flux circulations from the decay of numerous active regions months earlier. Additionally, our analysis suggests a potential link between the OMF enhancement and the concurrent emergence of the largest active region in solar cycle 24. In conclusion, our study provides insights into the strong increase in OMF observed during 2014 September–October.

Unified Astronomy Thesaurus concepts: Solar magnetic fields (1503); Solar physics (1476); Heliosphere (711)



Magnetograph Saturation and the Open Flux Problem

Y.-M. Wang¹ , R. K. Ulrich² , and J. W. Harvey^{3,4}

¹ Space Science Division, Naval Research Laboratory, Washington, DC 20375, USA; yi.wang@nrl.navy.mil

² Department of Physics and Astronomy, University of California, Los Angeles, CA 90095, USA; ulrich@astro.ucla.edu

³ National Solar Observatory, Boulder, CO 80303, USA; jharvey@nso.edu

Received 2021 November 22; revised 2021 December 17; accepted 2021 December 17; published 2022 February 17

Abstract

Extrapolations of line-of-sight photospheric field measurements predict radial interplanetary magnetic field (IMF) strengths that are factors of ~ 2 – 4 too low. To address this *open flux problem*, we reanalyze the magnetograph measurements from different observatories, with particular focus on those made in the saturation-prone Fe I 525.0 nm line by the Mount Wilson Observatory (MWO) and the Wilcox Solar Observatory (WSO). The total dipole strengths, which determine the total open flux, generally show large variations among observatories, even when their total photospheric fluxes are in agreement. However, the MWO and WSO dipole strengths, as well as their total fluxes, agree remarkably well with each other, suggesting that the two data sets require the same scaling factor. As shown earlier by Ulrich et al., the saturation correction δ^{-1} derived by comparing MWO measurements in the 525.0 nm line with those in the nonsaturating Fe I 523.3 nm line depends sensitively on where along the irregularly shaped 523.3 nm line wings the exit slits are placed. If the slits are positioned so that the 523.3 and 525.0 nm signals originate from the same height, $\delta^{-1} \sim 4.5$ at the disk center, falling to ~ 2 near the limb. When this correction is applied to either the MWO or WSO maps, the derived open fluxes are consistent with the observed IMF magnitude. Other investigators obtained scaling factors only one-half as large because they sampled the 523.3 nm line farther out in the wings, where the shift between the right- and left-circularly polarized components is substantially smaller.

Unified Astronomy Thesaurus concepts: Solar magnetic fields (1503); Interplanetary magnetic fields (824); Solar photosphere (1518); Solar chromosphere (1479); Solar coronal holes (1484); Solar cycle (1487); Stellar spectral lines (1630)

Interpretation of Solar Magnetic Field Strength Observations

R.K. Ulrich · L. Bertello · J.E. Boyden · L. Webster

Received: 29 August 2008 / Accepted: 11 December 2008 / Published online: 15 January 2009
© The Author(s) 2009. This article is published with open access at Springerlink.com

Abstract This study based on longitudinal Zeeman effect magnetograms and spectral line scans investigates the dependence of solar surface magnetic fields on the spectral line used and the way the line is sampled to estimate the magnetic flux emerging above the solar atmosphere and penetrating to the corona from magnetograms of the Mt. Wilson 150-foot tower synoptic program (MWO). We have compared the synoptic program $\lambda 5250 \text{ \AA}$ line of Fe I to the line of Fe I at $\lambda 5233 \text{ \AA}$ since this latter line has a broad shape with a profile that is nearly linear over a large portion of its wings. The present study uses five pairs of sampling points on the $\lambda 5233 \text{ \AA}$ line. Line profile observations show that the determination of the field strength from the Stokes V parameter or from line bisectors in the circularly polarized line profiles lead to similar dependencies on the spectral sampling of the lines, with the bisector method being the less sensitive. We recommend adoption of the field determined with the line bisector method as the best estimate of the emergent photospheric flux and further recommend the use of a sampling point as close to the line core as is practical. The combination of the line profile measurements and the cross-correlation of fields measured simultaneously with $\lambda 5250 \text{ \AA}$ and $\lambda 5233 \text{ \AA}$ yields a formula for the scale factor δ^{-1} that multiplies the MWO synoptic magnetic fields. By using ρ as the center-to-limb angle (CLA), a fit to this scale factor is $\delta^{-1} = 4.15 - 2.82 \sin^2(\rho)$. Previously $\delta^{-1} = 4.5 - 2.5 \sin^2(\rho)$ had been used. The new calibration shows that magnetic fields measured by the MDI system on the SOHO spacecraft are equal to 0.619 ± 0.018 times the true value at a center-to-limb position 30° . Berger and Lites (2003, *Solar Phys.* **213**, 213) found this factor to be 0.64 ± 0.013 based on a comparison using the Advanced Stokes Polarimeter.

Seventh Cambridge Workshop on Cool Stars, Stellar Systems, and the Sun
ASP Conference Series, Vol. 26, 1992
Mark S. Giampapa and Jay A. Bookbinder (eds.)

ANALYSIS OF MAGNETIC FLUXTUBES ON THE SOLAR SURFACE FROM OBSERVATIONS AT MT. WILSON OF $\lambda 5250$ AND $\lambda 5233$

ROGER K. ULRICH Department of Astronomy, University of California at Los Angeles, Los Angeles, CA 90024

ABSTRACT Simultaneous observations of $\lambda 5250$ and $\lambda 5233$ with spatial resolutions of $5'' \times 5''$, $12'' \times 12''$ and $20'' \times 20''$ have been used to determine a saturation factor which should be used to correct magnetic field measurements made with $\lambda 5250$. In contrast to previous results which gave a factor of roughly 2, the present determination which takes advantage of new flexibility in the Mt. Wilson system and is based on a very widely spaced separation of the spectral acceptance bands at $\lambda 5250$ yields a factor of roughly 4. This saturation factor depends on the spatial resolution and on the center-to-limb position.

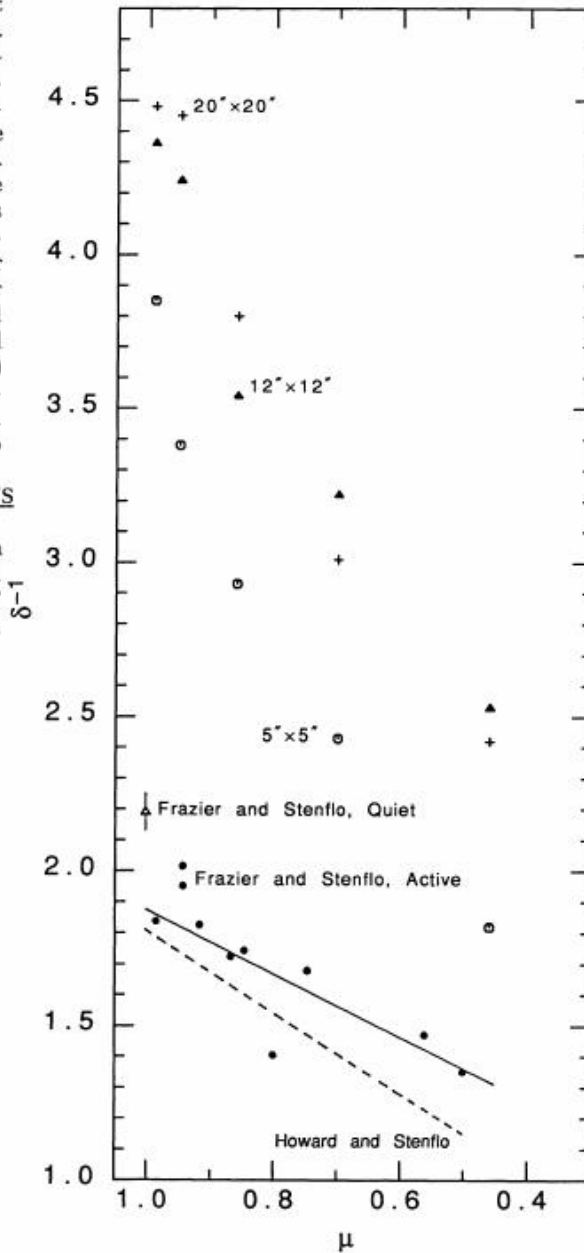
Keywords: Solar Magnetograms, Interplanetary Magnetic Fields, Magnetic Fluxtubes

Fig. 1. This figure shows the factor by which $\lambda 5250$ magnetic fields observed at Mt. Wilson should be multiplied in order to obtain unsaturated estimates which would have been measured at $\lambda 5233$. Note the aperture size dependence as well as the center-to-limb angle dependence. For comparison the earlier results by Frazier and Stenflo are shown (solid line and filled circles) as well as the summary relationship found by Howard and Stenflo (dashed line).

ACKNOWLEDGEMENTS

This work has been supported by NASA grant NAGW-472, NSF grant AST90-15108 and ONR:N00014 91-J114.

$\lambda 5250$ Reduction Factor



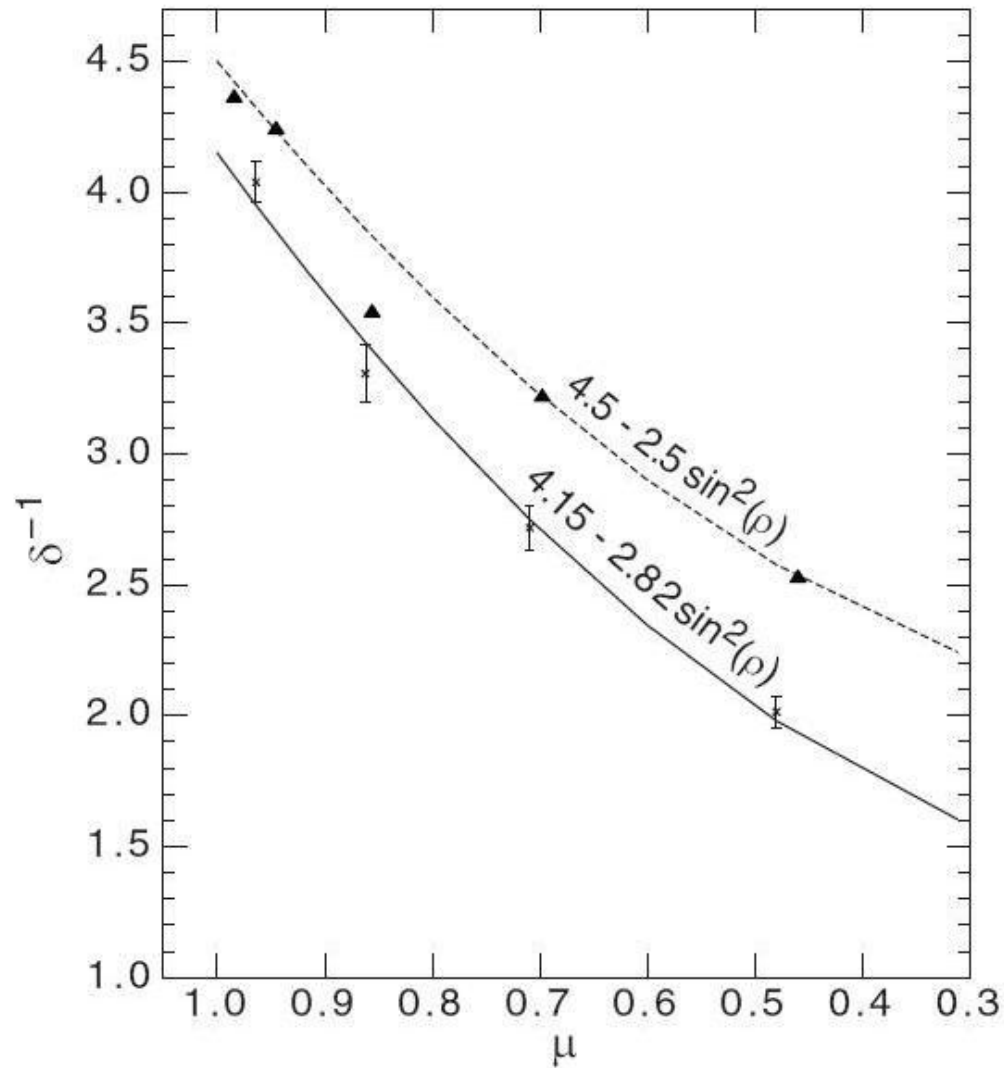


Figure 13. This figure shows the final scale factor δ^{-1} which converts the observed magnetic field for $\lambda 5250\text{\AA} \pm 39\text{m\AA}$ into the recommended magnetic field strength that gives our best estimate of the magnetic flux from each pixel emerging into the region above the solar atmosphere. The \times symbols with the error bars give the values of $\eta_{5233,84}^{5250,39}$ with their formal uncertainties multiplied by the average value of y of 0.73. The solid line is the fit to $\sin^2(\rho)$ with the fitting coefficients given above the line. In a similar fashion the filled triangles give the points from Ulrich (1992) with dashed line showing the fit to these points and the fitting coefficients in use by Wang and Sheeley (1995).

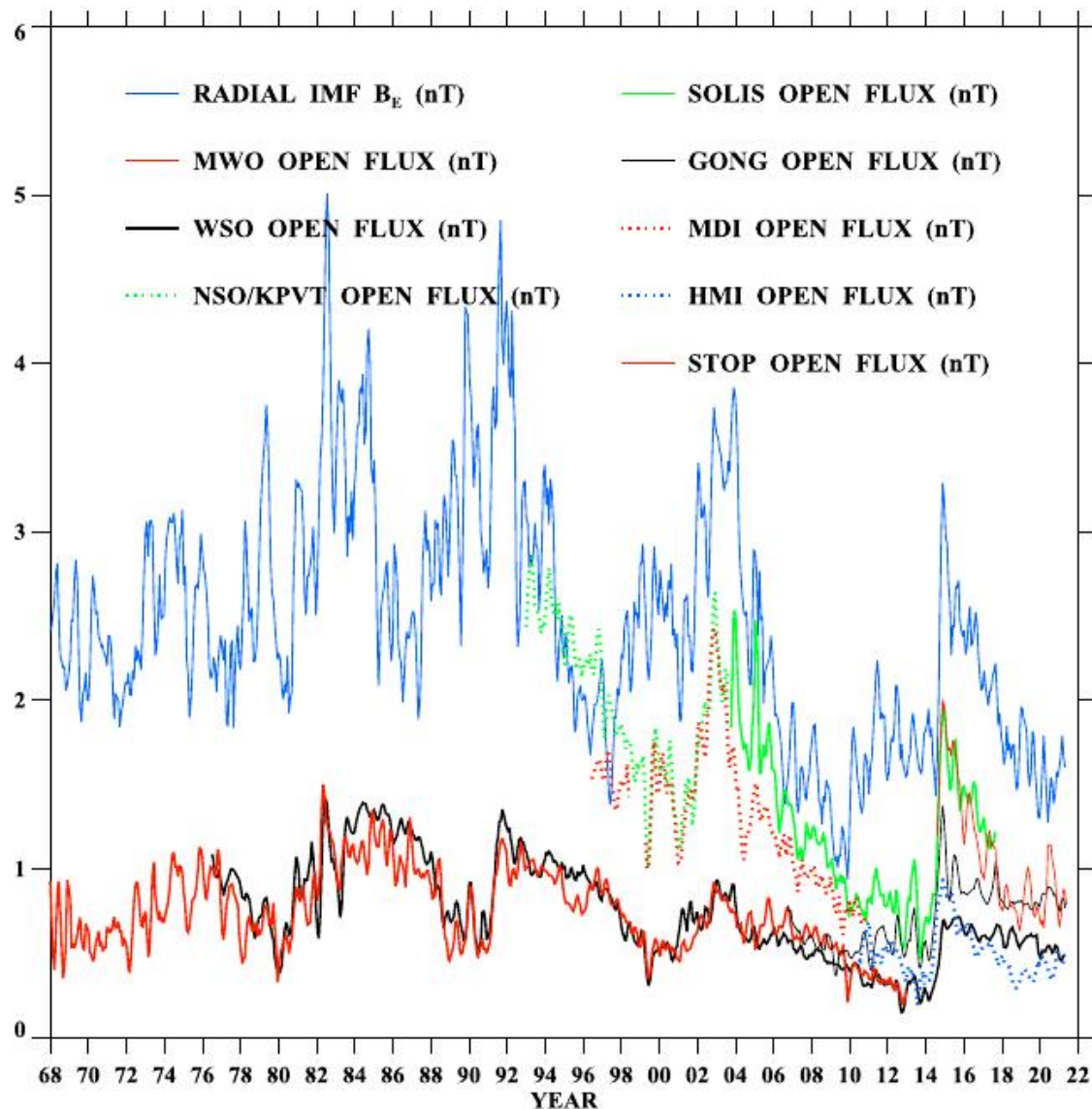


Figure 1. Comparison between the near-Earth radial IMF strength measured during 1968–2021 and the total open fluxes derived by applying a PFSS extrapolation to photospheric field maps from MWO, WSO, KPVT/SPM, SOLIS, GONG, MDI, HMI, and STOP. The source surface radius was fixed at $R_{ss} = 2.5 R_{\odot}$, B_r was matched to the photospheric field on the assumption that it is radially oriented, and the total unsigned flux crossing the source surface was converted into a field strength at 1 au by dividing by $4\pi r_E^2$. Daily values of B_r measured near Earth were extracted from the OMNIWeb database and averaged without the sign over successive CRs. The MWO and WSO maps were interpolated to 72 longitude pixels by 36 latitude pixels, while the remaining maps were regridded to dimensions of 360×180 ; no other corrections (other than for line-of-sight projection) were applied to the maps after downloading them from the observatory websites. Here and in the next three figures, all curves represent 3-CR running averages.

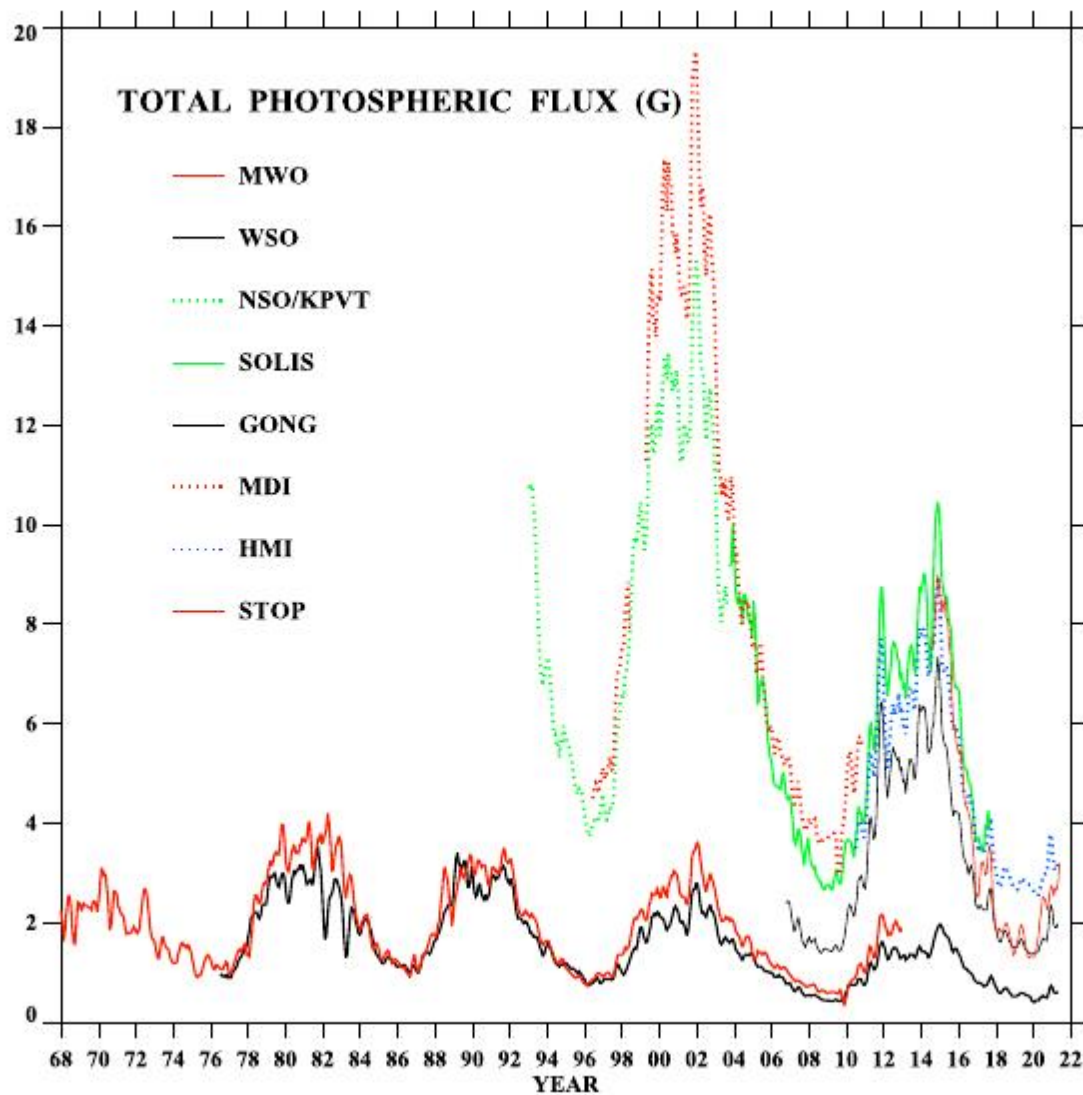


Figure 4. Variation of B_{tot} , the total unsigned photospheric flux averaged over the solar surface. Agreement between total fluxes may (as in the case of MWO and WSO) or may not (as in the case of SOLIS and HMI) entail agreement between open fluxes or dipole strengths (compare Figure 4 with Figures 1–3).

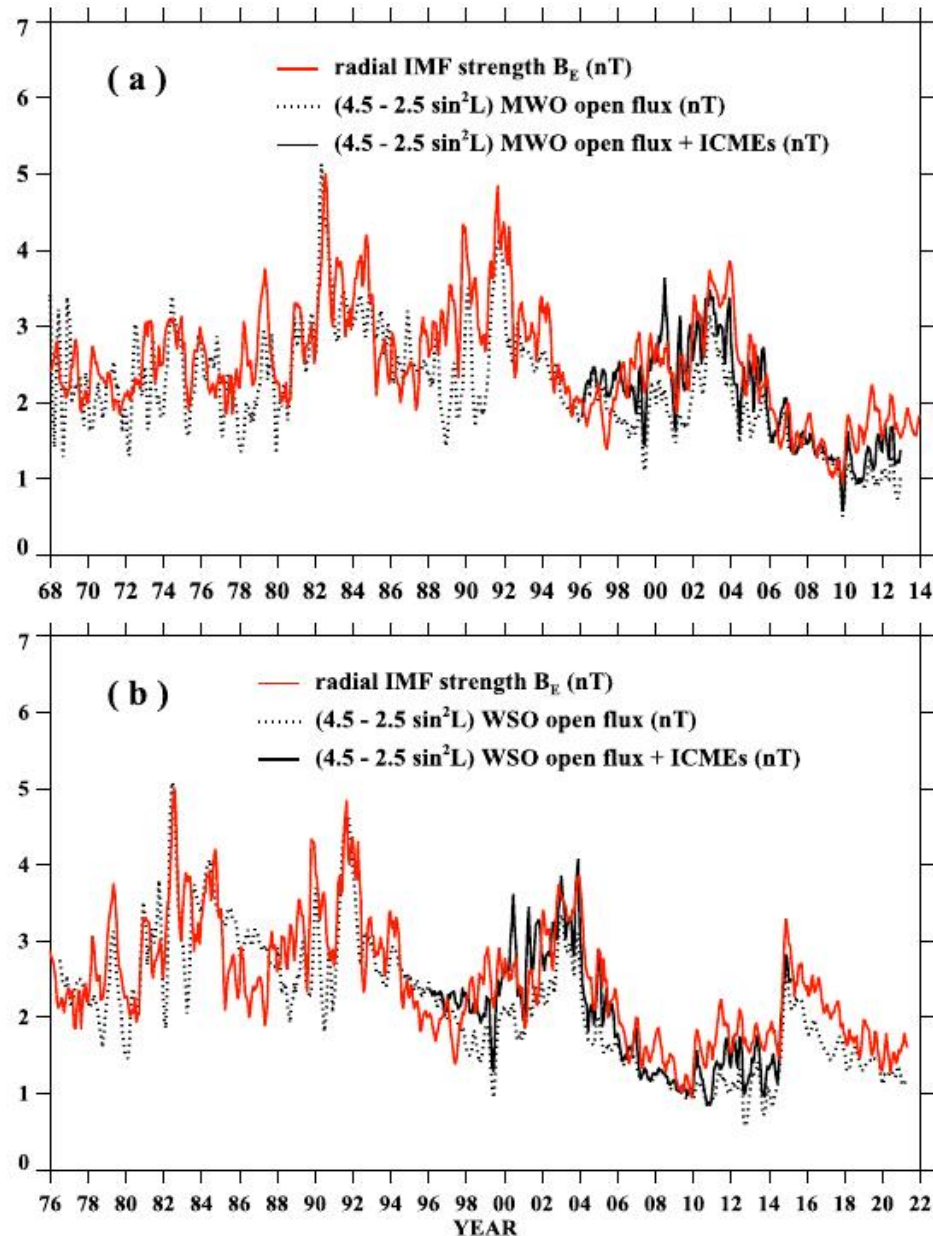
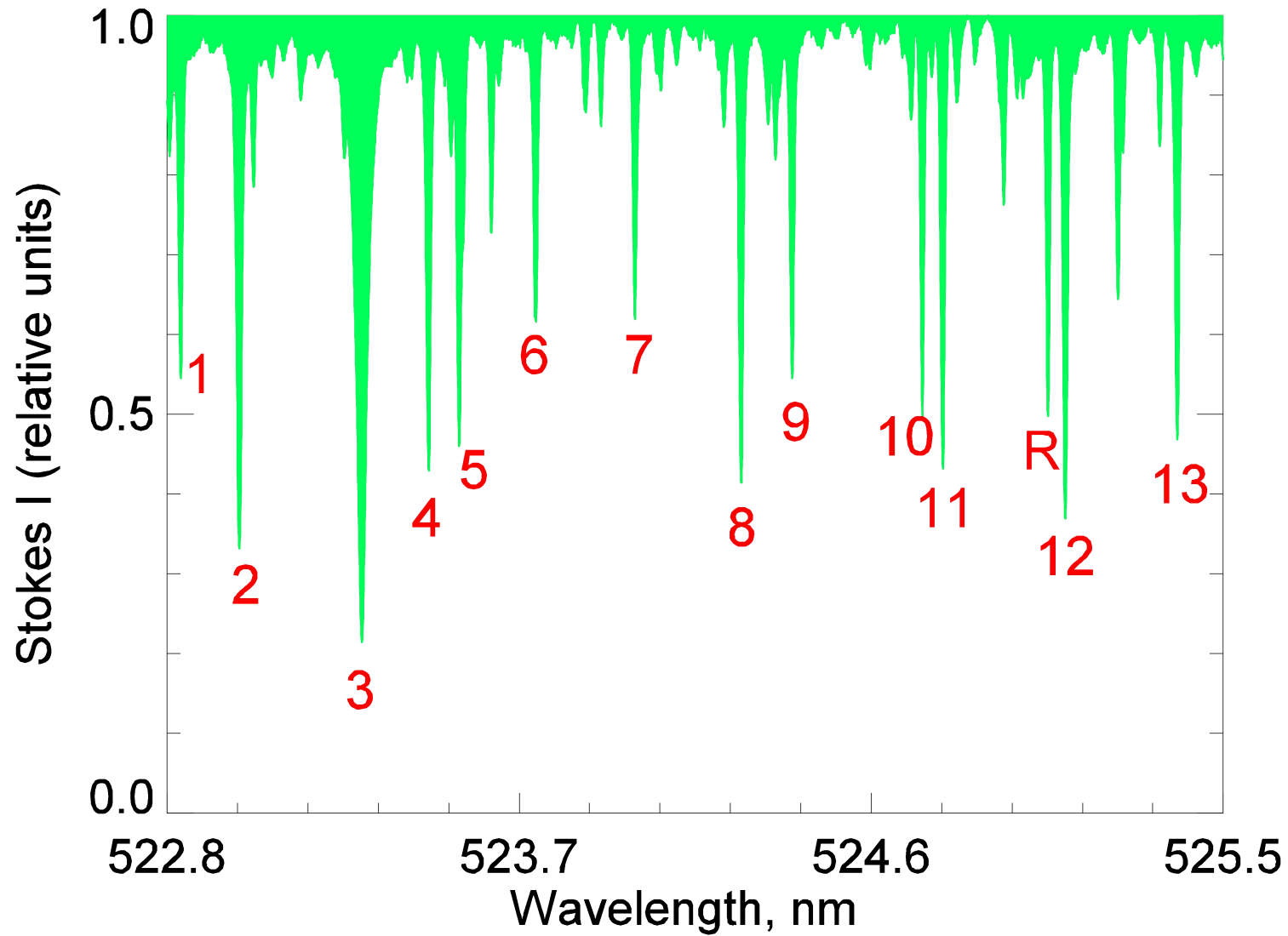
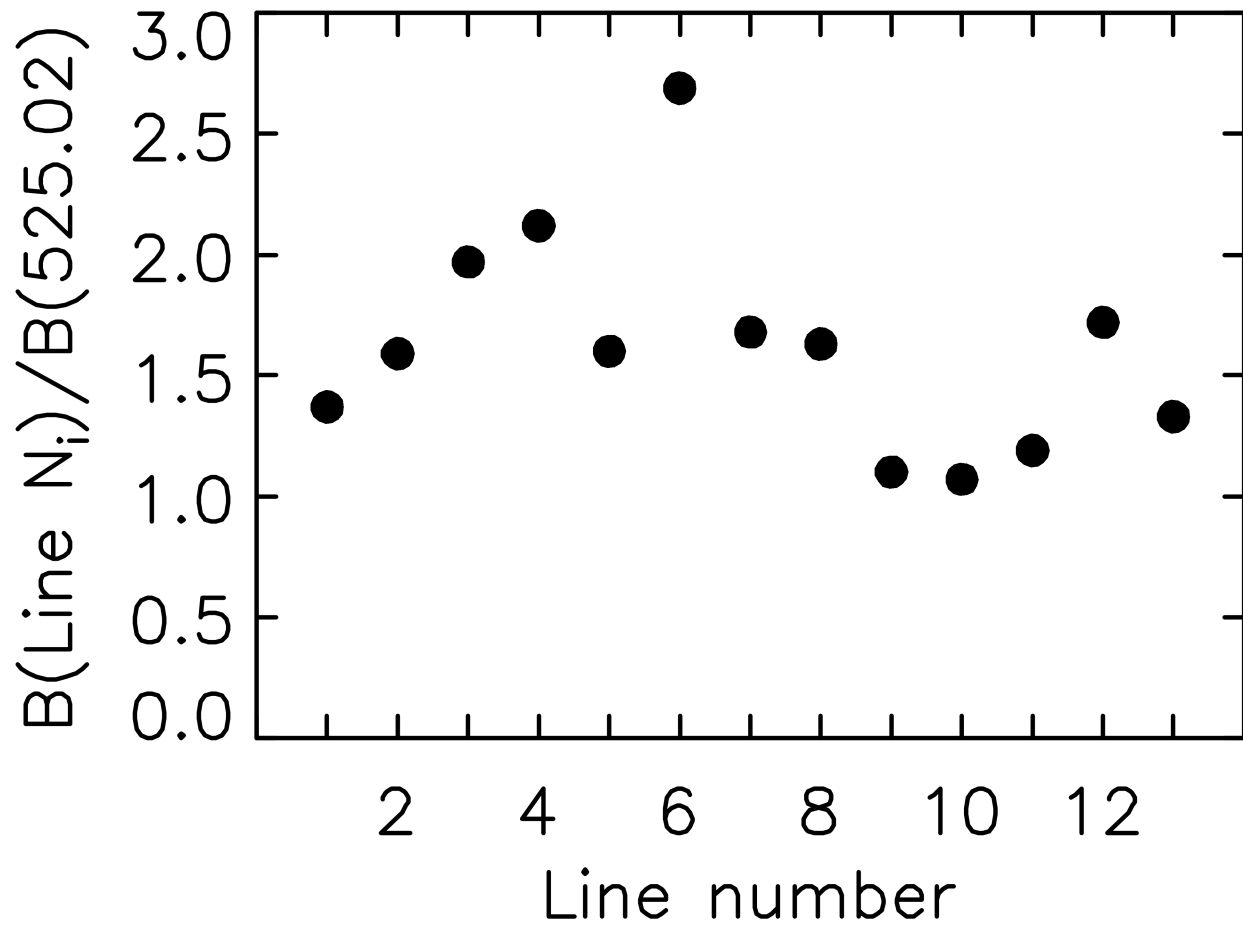
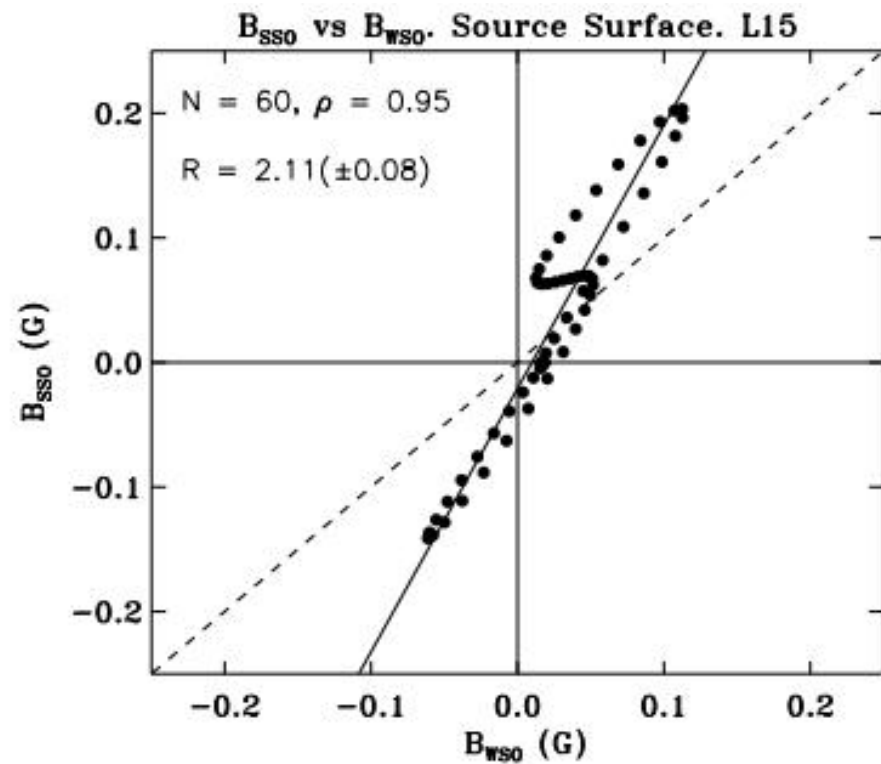
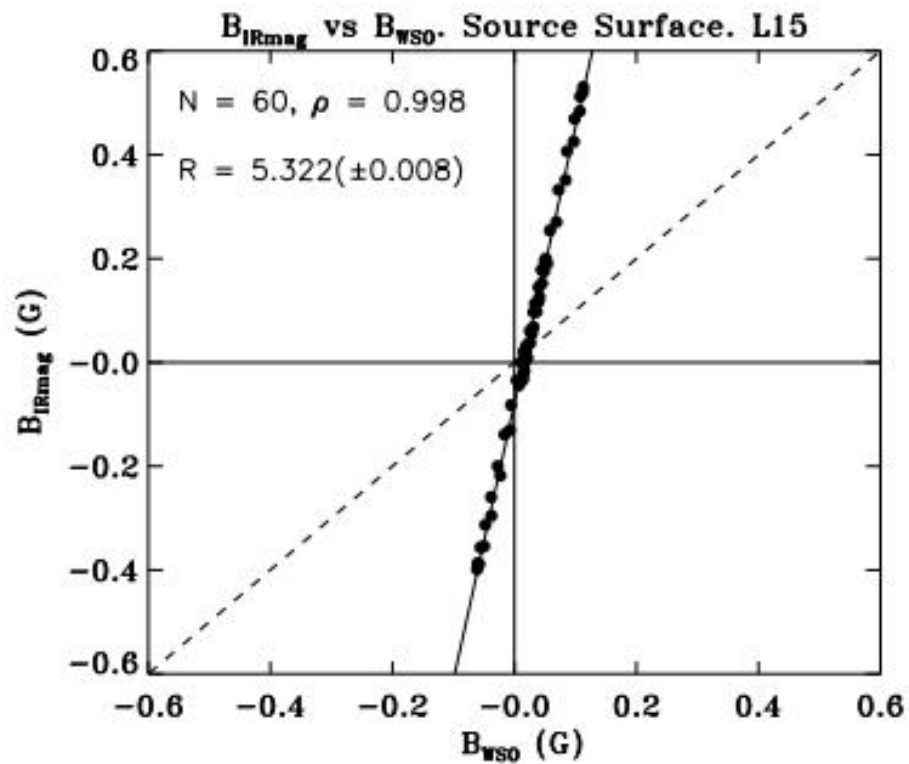


Figure 10. Effect of adding the contribution of ICMEs to the (a) MWO and (b) WSO total open fluxes, corrected using the $\delta^{-1} = (4.5 - 2.5 \sin^2 L)$ scaling factor. Near-Earth ICMEs during 1996–2015 were identified using the online Richardson–Cane catalog and assigned radial field strengths from the OMNIWeb database (see Wang & Sheeley 2015). ICMEs contributed $\sim 23\%$ of the interplanetary flux during 1999–2002 and $\sim 18\%$ during 2011–2014; their inclusion improves the agreement between the predicted and observed IMF strength during the rising and maximum phases of the solar cycle.

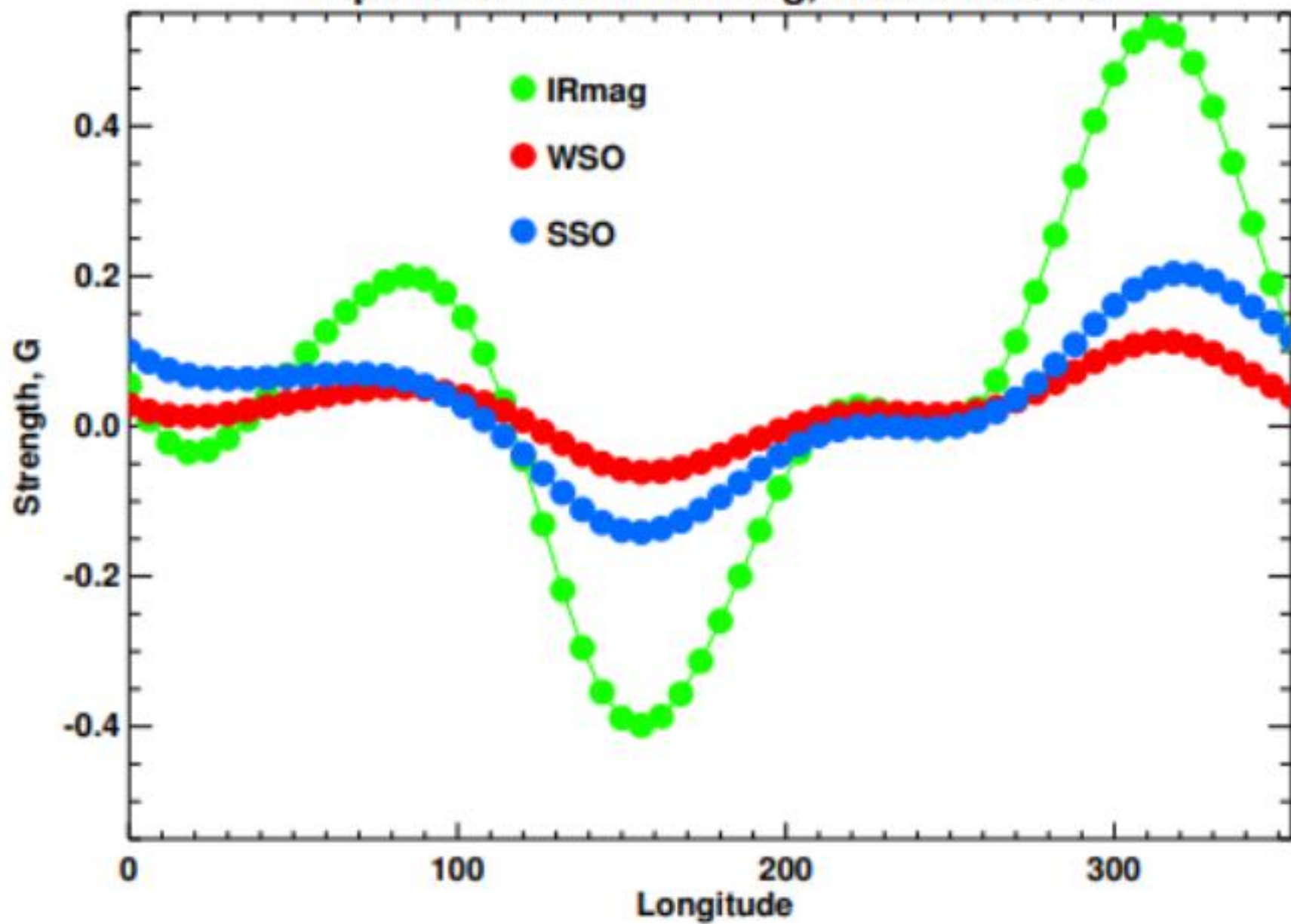
- Harvey, J. and Livingston, W. Sol.Ph. 22. 1969
- Howard, R., Stenflo, J.O. Sol.Ph. 22. 1972
- Stenflo, J.O. Sol.Ph. 1973
- Ulrich, R.K. PASP. 26. 1992
- Ulrich, R.K., et al., ApJS. 139. 2002
- Tran., T., et al., ApJS. 156. 2005.
- Martinez Gonzalez, M.J., et al. A&A. 456. 2006
- Socas-Navarro, H., et al. ApJ. 674. 2008
- Demidov, M.L., et al., Sol.Ph. 250. 2008
- Ulrich, R.K., et al. Sol.Ph. 255, 2009
- Demidov M.L., Balthasar, H. Sol.Ph. 260. 2009
- Stenflo, J.O. A&A, 517, 2010
- Stenflo, J.O. A&A. 529, 2011
- Demidov M.L., Balthasar, H. Sol.Ph. 276. 2012
- Balthasar, Demidov M.L., Sol.Ph. 276. 2012
- Riley, P., et al. Sol Ph. 2013
- Stenflo, J, O, et al, A&A. 556. 2013

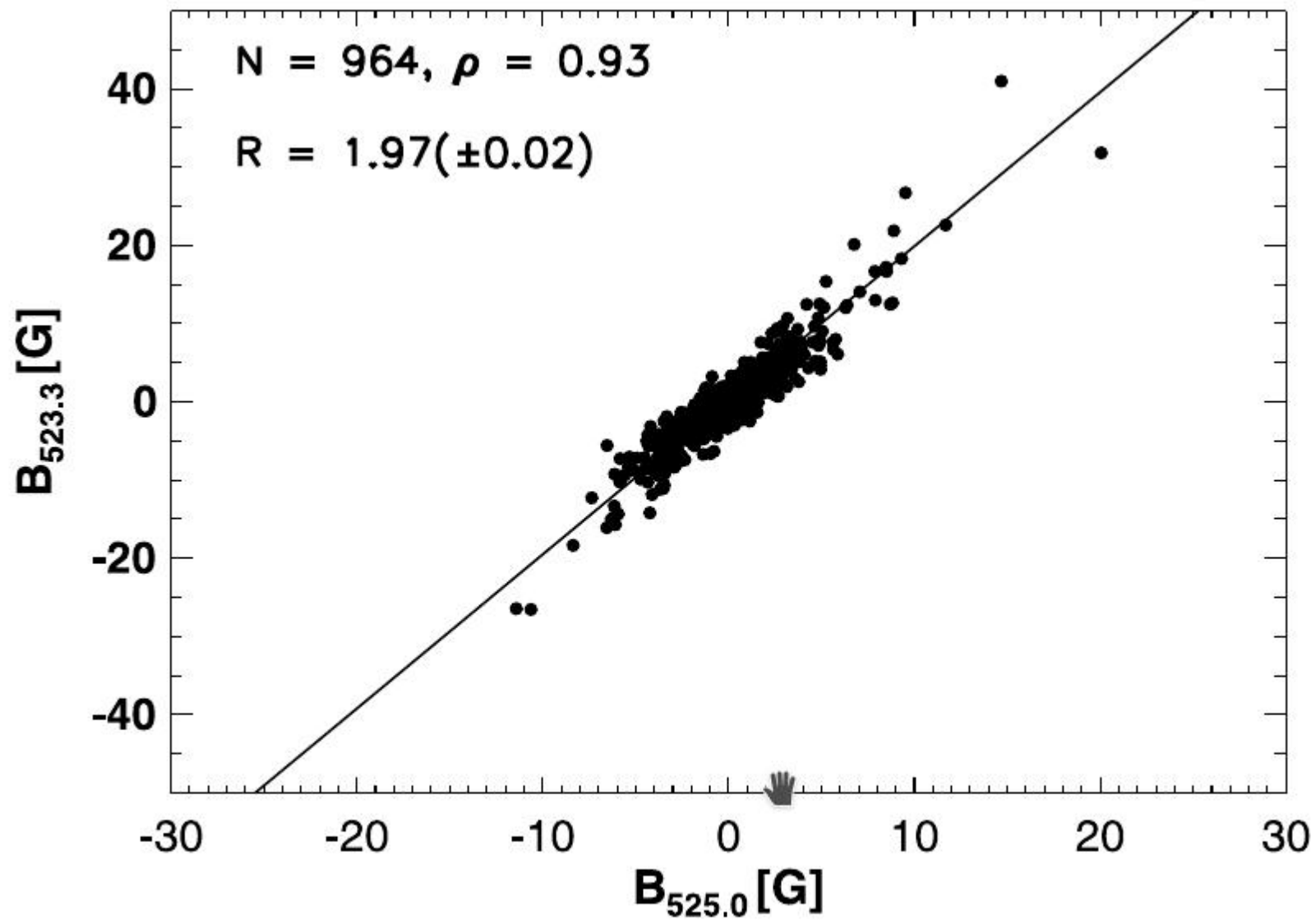


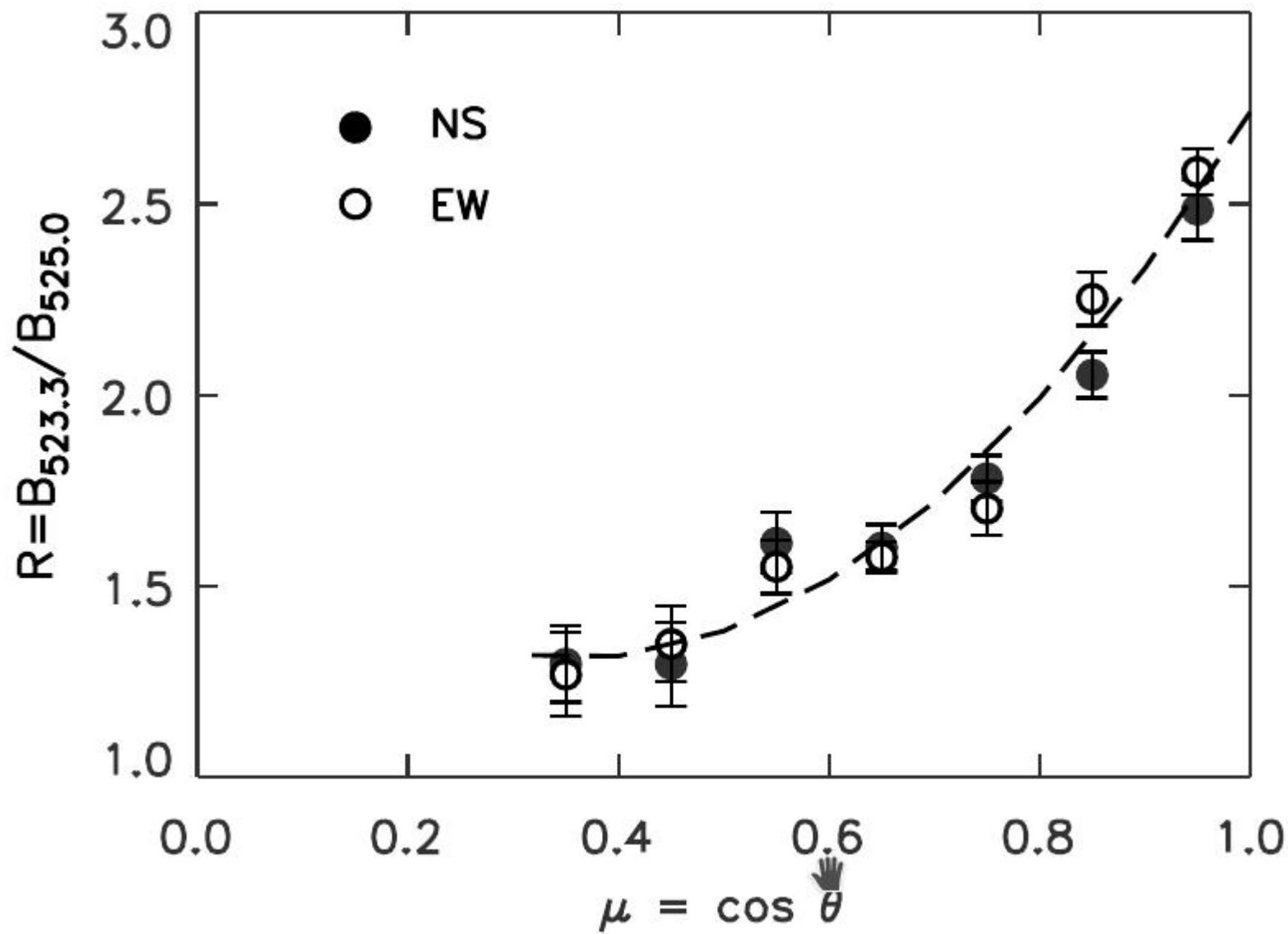




Equatorial Br from IRmag, WSO and SSO







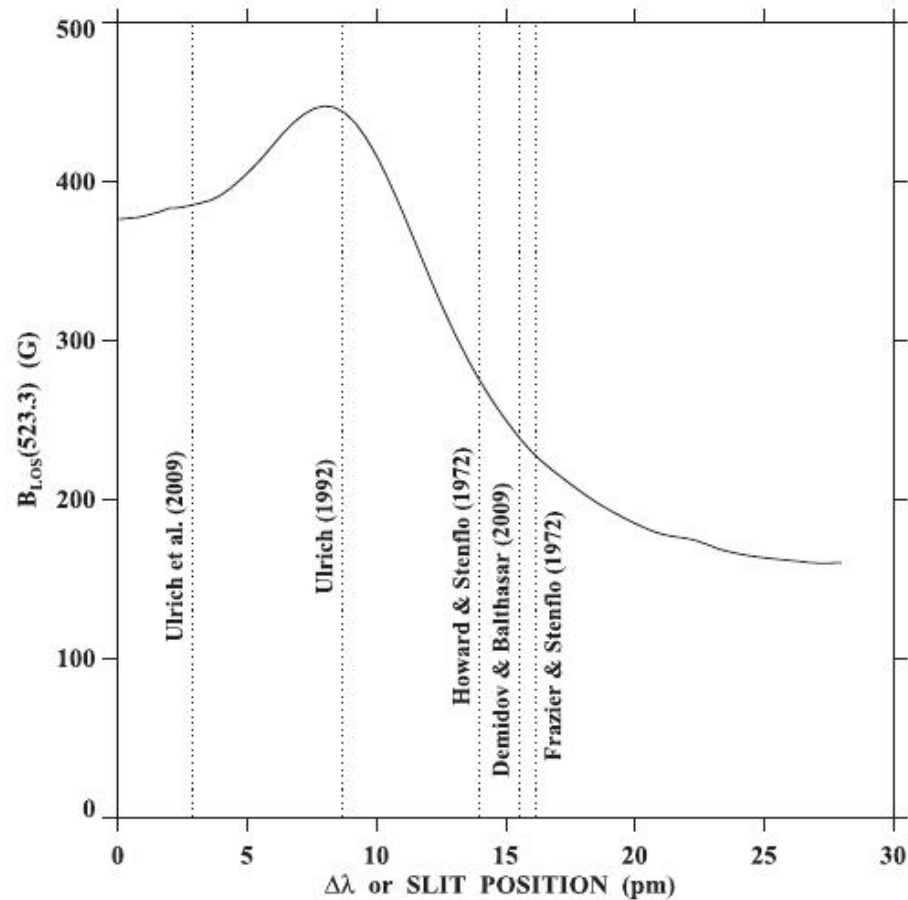
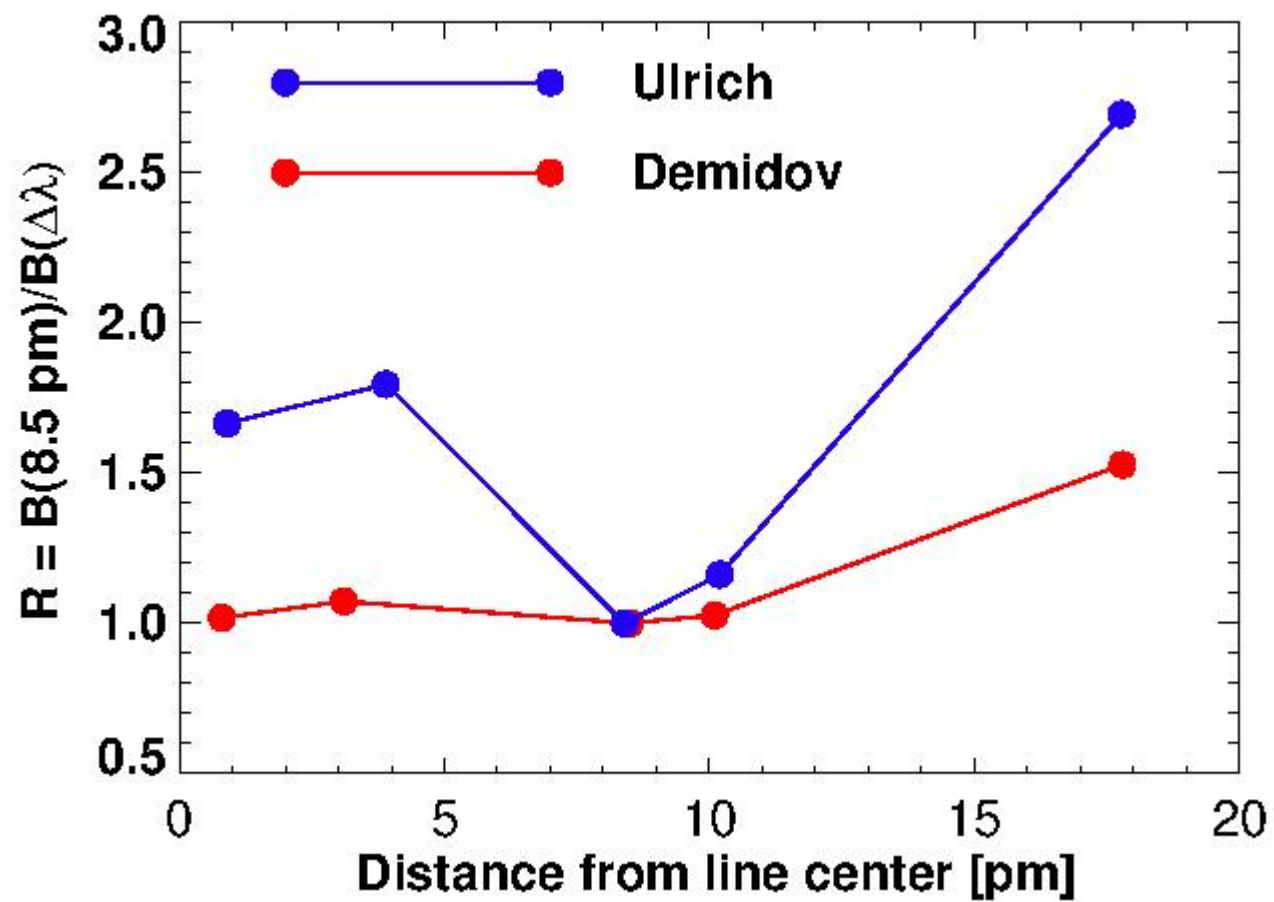
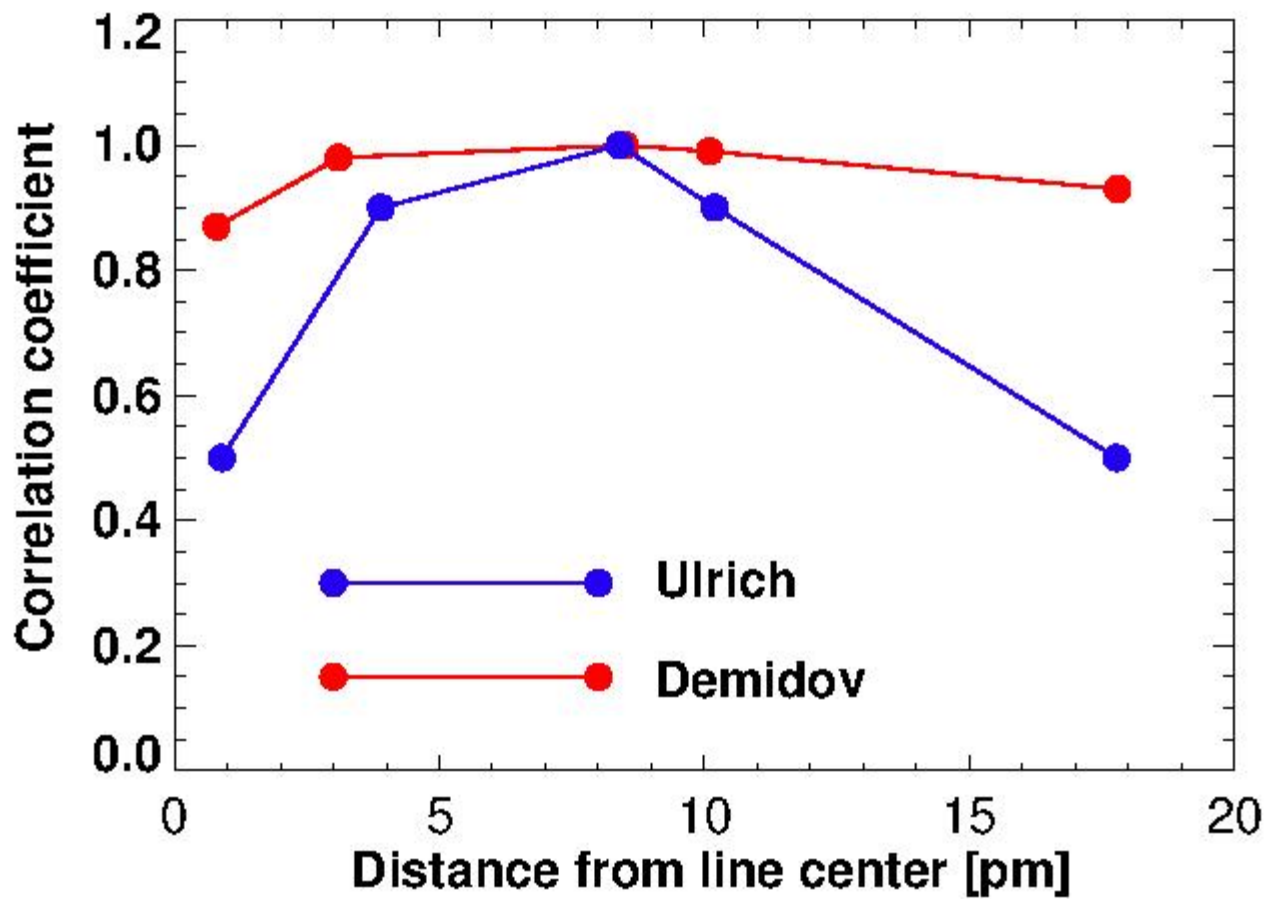
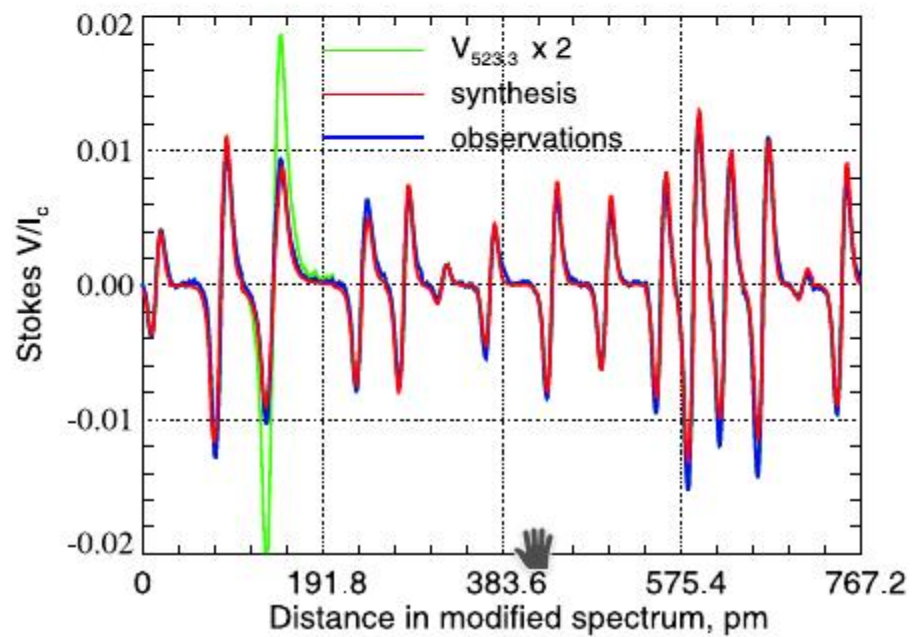
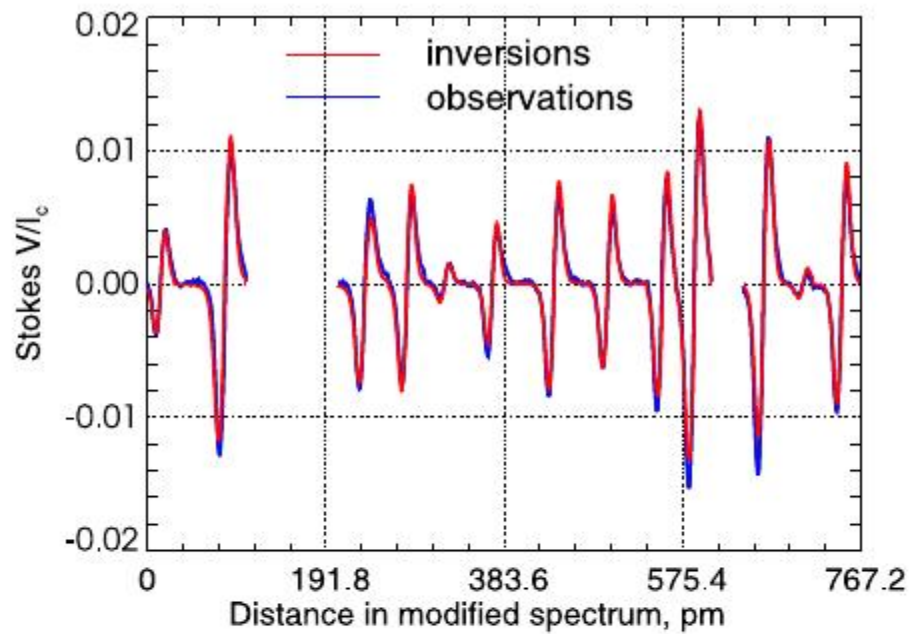


Figure 7. Derived field strength $B_{\text{los}}(523.3)$ as a function of $\Delta\lambda$, the wavelength position on the Fe I 523.3 nm line profile where the Zeeman shift is measured (using the line bisector method). The curve is reproduced from Figure 7 of Ulrich et al. (2009), and is based on left- and right-circularly polarized line profiles of a plage region observed with the MWO magnetograph on 2007 July 13. The vertical dotted lines mark the center positions of the exit slits used in the 523.3 nm measurements of Howard & Stenflo (1972), Frazier & Stenflo (1972), Ulrich (1992), Ulrich et al. (2009), and Demidov & Balthasar (2009). The curve peaks at $\Delta\lambda \sim 8$ pm, close to the slit position of Ulrich (1992). Howard & Stenflo, Frazier & Stenflo, and Demidov & Balthasar obtained lower values of $\delta^{-1} = B_{\text{los}}(523.3)/B_{\text{los}}(525.0)$ because they placed their slits farther out in the 523.3 nm line wings ($\Delta\lambda \sim 15$ pm), where $B_{\text{los}}(523.3)$ falls by a factor of order 2. The slits had total widths of 16 pm (Howard & Stenflo 1972), 17.5 pm (Frazier & Stenflo 1972), 5.0 pm (Ulrich 1992; Ulrich et al. 2009), and 24.84 pm (Demidov & Balthasar 2009).

$\Delta\lambda$ [pm]	Slit width W [pm]	ρ	$R = B(\pm 8.5 \text{ pm})/B(\pm \Delta\lambda)$
± 15.53	24.82	0.991	1.271 ± 0.009
± 0.8	0.80	0.870	1.018 ± 0.028
± 3.1	1.55	0.977	1.073 ± 0.013
± 10.1	9.32	0.998	1.027 ± 0.003
± 17.8	9.32	0.935	1.528 ± 0.030







Sergey Svertilov, Vitaly Bogomolov, Andery Bogomolov, Anatoly Iyudin, Vladimir Kalegaev, Vladislav Osedlo, Ivan Yashin. Monitoring of space weather effects with the use of Moscow University Sozvezdie-270 Nano-satellite Constellation. 47

Jingye Yan, Lin Wu, Li Deng, Xinhua Zhao, Mao Yuan, Xuning Lü, Yang Yang, Jiyao Xu, Ji Wu, Chi Wang. DART: Daocheng Radio Telescope system and early results 47

Yongqiang Yao, Xuan Qian. Environmental conditions at the high-altitude Ali observatory for space weather research 48

Yury Yasyukevich, Alexander Kiselev, Artem Vesnin, Artem Padokhin, Ilya Edemskiy, Alexander Ivanov, Boris Salimov. Global navigation satellite systems for space weather studies 48



谢谢

Thank you!

Спасибо!

